

# A Diagrammatic Approach to Improve Computational Efficiency in Group Equivariant Neural Networks

**Edward Pearce-Crump**

*Department of Computing  
Imperial College London  
London, SW7 2RH, United Kingdom*

EP1011@IMPERIAL.AC.UK

**William J. Knottenbelt**

*Department of Computing  
Imperial College London  
London, SW7 2RH, United Kingdom*

WJK@IMPERIAL.AC.UK

## Abstract

Group equivariant neural networks are growing in importance owing to their ability to generalise well in applications where the data has known underlying symmetries. Recent characterisations of a class of these networks that use high-order tensor power spaces as their layers suggest that they have significant potential; however, their implementation remains challenging owing to the prohibitively expensive nature of the computations that are involved. In this work, we present a fast matrix multiplication algorithm for any equivariant weight matrix that maps between tensor power layer spaces in these networks for four groups: the symmetric, orthogonal, special orthogonal, and symplectic groups. We obtain this algorithm by developing a diagrammatic framework based on category theory that enables us to not only express each weight matrix as a linear combination of diagrams but also makes it possible for us to use these diagrams to factor the original computation into a series of steps that are optimal. We show that this algorithm improves the Big- $O$  time complexity exponentially in comparison to a naïve matrix multiplication.

**Keywords:** deep learning theory, equivariant neural networks, weight matrices

## 1 Introduction

Incorporating symmetries as an inductive bias in neural network design has emerged as an important method for creating more structured and efficient models. These models, commonly referred to as *group equivariant neural networks* (Cohen and Welling, 2016, 2017; Qi et al., 2017; Ravanbakhsh et al., 2017; Zaheer et al., 2017; Cohen et al., 2018; Esteves et al., 2018; Kondor and Trivedi, 2018; Thomas et al., 2018; Maron et al., 2019a; Cohen et al., 2019; Weiler and Cesa, 2019; Villar et al., 2021; Finzi et al., 2021; Pearce-Crump, 2023a,b, 2024; Godfrey et al., 2023; Pearce-Crump and Knottenbelt, 2024), have proven to be useful across a wide range of applications, including, but not limited to, molecule generation (Satorras et al., 2021); designing proteins (Jumper et al., 2021); natural language processing (Gordon et al., 2020; Petrache and Trivedi, 2024); computer vision (Chatzipantazis et al., 2023); dynamics prediction (Guttenberg et al., 2016); and even auction design (Rahme et al., 2021).

Notably, several recent works have characterised the weight matrices of a class of group equivariant neural networks that use high-order tensor power spaces as their layers

(Ravanbakhsh et al., 2017; Maron et al., 2019a; Pearce-Crump, 2023a,b, 2024; Godfrey et al., 2023; Pearce-Crump and Knottenbelt, 2024). However, because these layers are tensor power spaces, the computations that are involved — specifically, applying an equivariant weight matrix to an input vector to transform it to an output vector — can be very expensive. Indeed, if the weight matrix is a function  $(\mathbb{R}^n)^{\otimes k} \rightarrow (\mathbb{R}^n)^{\otimes l}$ , then a naïve matrix multiplication on an input vector  $v \in (\mathbb{R}^n)^{\otimes k}$  has a time complexity of  $O(n^{l+k})$ . Hence there is a need to develop methods that make these computations feasible in practice so that the networks that use these weight matrices become more efficient.

We address this problem in the following way, for four groups whose weight matrices have been characterised previously: the symmetric (Ravanbakhsh et al., 2017; Maron et al., 2019a; Pearce-Crump, 2024; Godfrey et al., 2023), orthogonal, special orthogonal and symplectic groups (Pearce-Crump, 2023a). We first develop a diagrammatic framework based on category theory, enabling us to express each group equivariant weight matrix as the image under a monoidal functor of a linear combination of morphisms in a diagram category. In this way, we can effectively interpret the morphisms in each diagram category as being equivalent to matrices. We then use the diagrammatic framework to develop an algorithm that improves upon the naïve weight matrix multiplication *exponentially* in terms of its Big- $O$  time complexity. We achieve this by using the diagrams that are equivalent to the original weight matrix to factor it into a sequence of operations that carry out the original calculation in the most efficient way possible. We suggest that our result might enable more widespread adoption of group equivariant neural networks that use high-order tensor power spaces in practical applications.

The rest of the paper is organised as follows. After discussing the related work in Section 2, we review in Section 3 the important concepts behind the characterisation of the equivariant weight matrices between tensor power spaces of  $\mathbb{R}^n$  that have appeared elsewhere in the literature. In Section 4, we introduce our diagrammatic framework that is based on category theory, to show that each linear map that we review in Section 3 is actually the result of a monoidal functor between a diagram category and a representation category. In particular, we conclude that section by discussing some fundamental results that form the basis of our main contribution, which is introduced in Section 5: the fast multiplication algorithm for passing a vector through an equivariant weight matrix for the four groups in question. In this section, we present our algorithm, discuss its implementation for each of the four groups, and analyse its Big- $O$  time complexity in each case. Finally, we conclude in Section 6.

## 2 Related Work

There is a growing body of literature demonstrating the application of category theory in machine learning. A number of works have used a category-theoretic approach either to construct, categorise, or analyse neural network architectures (Gavranović et al., 2024; Abbott, 2024; Khatri et al., 2024; Tull et al., 2024). Some researchers have explored expanding the concept of equivariance through category theory, resulting in new insights on the structure of equivariant models (de Haan et al., 2020; Gavranović et al., 2024) while others have focused on understanding gradient-based learning using a category-theoretic framework (Cruttwell et al., 2022). Additionally, recent works have examined stochas-

tic equivariant models (Cho and Jacobs, 2019; Bloem-Reddy and Teh, 2020; Fritz, 2020; Cornish, 2024) and causal reasoning (Lorenz and Tull, 2023) within the context of Markov categories. Building on these works, we adopt a category-theoretic approach to gain insights into the construction of specific neural networks; namely, the weight matrices of certain tensor power based equivariant neural networks. The primary distinction and contribution of our work lies in using this approach not only to understand the construction of the neural networks themselves but also to significantly improve the time complexity of the forward pass that is involved in their execution.

Finally, in a loosely-related body of work, there is a whole subdomain in quantum computing where formal category-theoretic languages, such as the ZX-calculus, are used to rewrite quantum circuits for compilation onto quantum hardware (Coecke and Kissinger, 2017; Duncan et al., 2020; Kissinger, 2012; Heunen and Vicary, 2020; van de Wetering, 2020). In this context, the original circuit needs to be rewritten in terms of a predefined set of quantum gates that is tailored to the specific quantum hardware. In our work, the algorithm that we present in Section 5 rewrites the equivariant weight matrix as a composition of operations; however, this algorithm is designed for classical computing, not quantum computing, and we focus on the time complexity of the operations involved, rather than the underlying hardware on which they will be executed.

### 3 Background

In this section, we revisit the concepts that led to the characterisation of the equivariant weight matrices between high-order tensor power spaces of  $\mathbb{R}^n$ , focusing on the four groups in question:  $S_n$ ,  $O(n)$ ,  $SO(n)$  and  $Sp(n)$ . This section is organised into three parts: first we recall the layer spaces, considered as representations of each group, and the definition of an equivariant map between them; second, we review the diagrams that were used to derive the weight matrix characterisations; and finally we summarise the key results, providing references to where their proofs can be found in the literature.

In the following, we write  $G(n)$  to refer to any of  $S_n$ ,  $O(n)$ ,  $SO(n)$  and  $Sp(n)$ . We consider  $G(n)$  to be a subgroup of matrices in  $GL(n)$  throughout, having chosen the standard basis of  $\mathbb{R}^n$ . We also write  $[n]$  for the set  $\{1, \dots, n\}$ , and  $[n]^p$  for the  $p$ -fold Cartesian product of the set  $\{1, \dots, n\}$ .

#### 3.1 Layer Spaces as Group Representations

For each neural network that is equivariant to  $G(n)$ , the layer spaces are not just vector spaces, they are representations of  $G(n)$ . This makes it possible to incorporate the symmetries as an inductive bias into the network not only through the action of the group on each layer space but also through the equivariant maps between them. We define each of these concepts in turn.

Each layer space is a high-order tensor power of  $\mathbb{R}^n$ , denoted  $(\mathbb{R}^n)^{\otimes k}$ , that comes with a representation of  $G(n)$ . This representation, written  $\rho_k : G(n) \rightarrow GL((\mathbb{R}^n)^{\otimes k})$ , is defined on the standard basis of  $(\mathbb{R}^n)^{\otimes k}$

$$e_I := e_{i_1} \otimes e_{i_2} \otimes \dots \otimes e_{i_k} \tag{1}$$

for all  $I := (i_1, i_2, \dots, i_k) \in [n]^k$  by

$$g \cdot e_I := ge_{i_1} \otimes ge_{i_2} \otimes \dots \otimes ge_{i_k} \quad (2)$$

and is extended linearly on the basis elements of  $(\mathbb{R}^n)^{\otimes k}$ .

We note that if  $G(n) = Sp(n)$ , then  $n = 2m$ , and we label and order the indices by  $1, 1', \dots, m, m'$  instead. In this case, we sometimes call the standard basis of  $\mathbb{R}^n$  the symplectic basis.

There is a special class of maps between representations of a group that are known as equivariant maps. Recall that a map  $\phi : (\mathbb{R}^n)^{\otimes k} \rightarrow (\mathbb{R}^n)^{\otimes l}$  between two representations of  $G(n)$  is said to be  $G(n)$ -equivariant if

$$\phi(\rho_k(g)[v]) = \rho_l(g)[\phi(v)] \quad (3)$$

for all  $g \in G(n)$  and  $v \in (\mathbb{R}^n)^{\otimes k}$ . We denote the vector space of all *linear*  $G(n)$ -equivariant maps between  $(\mathbb{R}^n)^{\otimes k}$  and  $(\mathbb{R}^n)^{\otimes l}$  by  $\text{Hom}_{G(n)}((\mathbb{R}^n)^{\otimes k}, (\mathbb{R}^n)^{\otimes l})$ .

We are interested in the equivariant weight matrices that map between any two adjacent layer spaces. It is clear that the equivariant weight matrices mapping  $(\mathbb{R}^n)^{\otimes k}$  to  $(\mathbb{R}^n)^{\otimes l}$  can be found by obtaining either a basis or a spanning set of matrices for  $\text{Hom}_{G(n)}((\mathbb{R}^n)^{\otimes k}, (\mathbb{R}^n)^{\otimes l})$ . The diagrams that can be used to obtain such a basis or spanning set form the topic of the next section.

### 3.2 Set Partition Diagrams

There are potentially a number of different ways to obtain such a basis or spanning set of matrices for each group. For example, for the symmetric group  $S_n$ , Maron et al. (2019a) considered so-called fixed-point equations to obtain a basis of matrices known as the orbit basis, and Godfrey et al. (2023) constructed an  $\mathbb{R}$ -algebra from the  $S_n$ -invariant subspace for each tensor power space of  $\mathbb{R}^n$  to obtain a different basis of matrices known as the diagram basis. We focus, however, on using set partition diagrams, which originally appeared in Pearce-Crump (2023a, 2024), as they serve as the foundation for our contributions that appear in the upcoming sections.

To introduce these diagrams, we need to begin with the definition of a set partition.

**Definition 1** *For any non-negative integers  $l$  and  $k$ , consider the set  $[l+k] := \{1, \dots, l+k\}$ . A **set partition**  $\pi$  of  $[l+k]$  is a partition of  $[l+k]$  into a disjoint union of subsets, each of which we call a **block**.*

**Example 1** *If  $l = 4$  and  $k = 6$ , then*

$$\{1, 2, 5, 7 \mid 3, 4, 10 \mid 6, 8 \mid 9\} \quad (4)$$

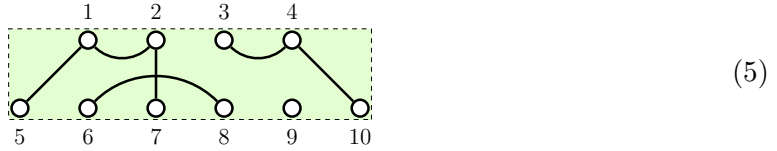
*is a set partition of  $[4+6]$  having 4 blocks.*

**Definition 2** *Let  $\pi$  be a set partition of  $[l+k]$ . We can associate to  $\pi$  a diagram  $d_\pi$ , called a  **$(k, l)$ -partition diagram**, that consists of two rows of vertices and edges between vertices such that there are*

- $l$  vertices on the top row, labelled left to right by  $1, \dots, l$
- $k$  vertices on the bottom row, labelled left to right by  $l + 1, \dots, l + k$ , and
- the edges between the vertices correspond to the connected components of  $\pi$ .

As a result,  $d_\pi$  represents the equivalence class of all diagrams with connected components equal to the blocks of  $\pi$ .

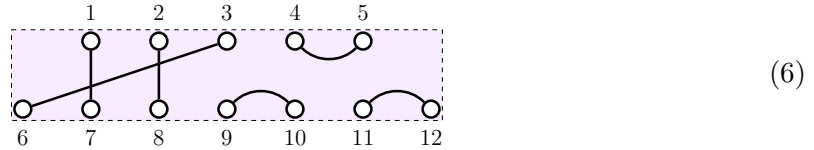
**Example 2** The  $(6, 4)$ -partition diagram corresponding to the set partition given in Example 1 is



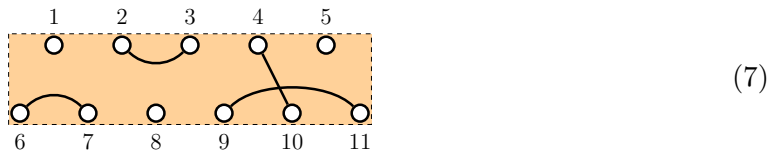
**Definition 3** We are also interested in the following types of  $(k, l)$ -partition diagrams.

- A  $(k, l)$ -**Brauer diagram**  $d_\beta$  is a  $(k, l)$ -partition diagram where the size of every block in  $\beta$  is exactly two.
- Given  $k$  and  $l$ , an  $(l + k) \setminus n$ -**diagram**  $d_\alpha$  is a  $(k, l)$ -partition diagram where exactly  $n$  blocks in  $\alpha$  have size one, with the rest having exactly size two. The vertices corresponding to the blocks of size one are called **free** vertices.

**Example 3** The first diagram below is a  $(7, 5)$ -Brauer diagram



whereas the second is a  $(5 + 6) \setminus 3$ -diagram



In order to state the characterisations more succinctly in the next section, we introduce a number of vector spaces as the formal  $\mathbb{R}$ -linear span of certain subsets of  $(k, l)$ -partition diagrams, as follows.

**Definition 4**

- The **partition vector space**  $P_k^l(n)$  is defined to be the  $\mathbb{R}$ -linear span of the set of all  $(k, l)$ -partition diagrams.
- The **Brauer vector space**  $B_k^l(n)$  is defined to be the  $\mathbb{R}$ -linear span of the set of all  $(k, l)$ -Brauer diagrams.
- The **Brauer-Grood vector space**  $D_k^l(n)$  is defined to be the  $\mathbb{R}$ -linear span of the set of all  $(k, l)$ -Brauer diagrams together with the set of all  $(l + k) \setminus n$ -diagrams.

### 3.3 Characterisation of Equivariant Weight Matrices

We now use the vector spaces given in Definition 4 to summarise the equivariant weight matrix characterisation results for each of the four groups. We state each basis/spanning set result as a theorem, and give its associated equivariant weight matrix characterisation as a corollary.

In order to state the results, recall that, for all non-negative integers  $l, k$ , the vector space of matrices  $\text{Hom}((\mathbb{R}^n)^{\otimes k}, (\mathbb{R}^n)^{\otimes l})$  has a standard basis of matrix units

$$\{E_{I,J}\}_{I \in [n]^l, J \in [n]^k} \quad (8)$$

where  $I$  is a tuple  $(i_1, i_2, \dots, i_l) \in [n]^l$ ,  $J$  is a tuple  $(j_1, j_2, \dots, j_k) \in [n]^k$  and  $E_{I,J}$  has a 1 in the  $(I, J)$  position and is 0 elsewhere.

**Theorem 5 (Diagram Basis when  $G(n) = S_n$ )** (Godfrey et al., 2023, Theorem 5.4)

For all non-negative integers  $l, k$  and any positive integer  $n$ , there is a surjection of vector spaces

$$\Theta_{k,n}^l : P_k^l(n) \rightarrow \text{Hom}_{S_n}((\mathbb{R}^n)^{\otimes k}, (\mathbb{R}^n)^{\otimes l}) \quad (9)$$

that is given by

$$d_\pi \mapsto D_\pi \quad (10)$$

for all  $(k, l)$ -partition diagrams  $d_\pi$ , where  $D_\pi$  is defined as follows. If  $S_\pi((I, J))$  is defined to be the set

$$\{(I, J) \in [n]^{l+k} \mid \text{if } x, y \text{ are in the same block of } \pi, \text{ then } i_x = i_y\} \quad (11)$$

(where we have momentarily replaced the elements of  $J$  by  $i_{l+m} := j_m$  for all  $m \in [k]$ ), then we have that

$$D_\pi := \sum_{I \in [n]^l, J \in [n]^k} \delta_{\pi, (I, J)} E_{I, J} \quad (12)$$

where

$$\delta_{\pi, (I, J)} := \begin{cases} 1 & \text{if } (I, J) \in S_\pi((I, J)) \\ 0 & \text{otherwise} \end{cases} \quad (13)$$

In particular, the set

$$\{D_\pi \mid d_\pi \text{ is a } (k, l)\text{-partition diagram having at most } n \text{ blocks}\} \quad (14)$$

is a basis for  $\text{Hom}_{S_n}((\mathbb{R}^n)^{\otimes k}, (\mathbb{R}^n)^{\otimes l})$  in the standard basis of  $\mathbb{R}^n$ , of size  $B(l+k, n) := \sum_{t=1}^n \binom{l+k}{t}$ , where  $\binom{l+k}{t}$  is the Stirling number of the second kind.

**Corollary 6 (Permutation Equivariant Weight Matrices)** For all non-negative integers  $l, k$  and positive integers  $n$ , the weight matrix  $W$  that appears in an  $S_n$ -equivariant linear layer function from  $(\mathbb{R}^n)^{\otimes k}$  to  $(\mathbb{R}^n)^{\otimes l}$  must be of the form

$$W = \sum_{d_\pi \in P_k^l(n)} \lambda_\pi D_\pi \quad (15)$$

**Theorem 7 (Spanning set when  $G(n) = O(n)$ )** (Pearce-Crump, 2023a, Theorem 6.5)

For all non-negative integers  $l, k$  and any positive integer  $n$ , there is a surjection of vector spaces

$$\Phi_{k,n}^l : B_k^l(n) \rightarrow \text{Hom}_{O(n)}((\mathbb{R}^n)^{\otimes k}, (\mathbb{R}^n)^{\otimes l}) \quad (16)$$

that is given by

$$d_\beta \mapsto E_\beta \quad (17)$$

for all  $(k, l)$ -Brauer diagrams  $d_\beta$ , where  $E_\beta := D_\beta$  is given in (12). In particular, the set

$$\{E_\beta \mid d_\beta \text{ is a } (k, l)\text{-Brauer diagram}\} \quad (18)$$

is a spanning set for  $\text{Hom}_{O(n)}((\mathbb{R}^n)^{\otimes k}, (\mathbb{R}^n)^{\otimes l})$  in the standard basis of  $\mathbb{R}^n$ , of size 0 when  $l + k$  is odd, and of size  $(l + k - 1)!!$  when  $l + k$  is even.

**Corollary 8 (Orthogonal Group Equivariant Weight Matrices)** For all non-negative integers  $l, k$  and positive integers  $n$ , the weight matrix  $W$  that appears in an  $O(n)$ -equivariant linear layer function from  $(\mathbb{R}^n)^{\otimes k}$  to  $(\mathbb{R}^n)^{\otimes l}$  must be of the form

$$W = \sum_{d_\beta \in B_k^l(n)} \lambda_\beta E_\beta \quad (19)$$

**Theorem 9 (Spanning set when  $G(n) = Sp(n), n = 2m$ )** (Pearce-Crump, 2023a, Theorem 6.6)

For all non-negative integers  $l, k$  and any positive integer  $n$  such that  $n = 2m$ , there is a surjection of vector spaces

$$X_{k,n}^l : B_k^l(n) \rightarrow \text{Hom}_{Sp(n)}((\mathbb{R}^n)^{\otimes k}, (\mathbb{R}^n)^{\otimes l}) \quad (20)$$

that is given by

$$d_\beta \mapsto F_\beta \quad (21)$$

for all  $(k, l)$ -Brauer diagrams  $d_\beta$ , where  $F_\beta$  is defined as follows.

Associate the indices  $i_1, i_2, \dots, i_l$  with the vertices in the top row of  $d_\beta$ , and  $j_1, j_2, \dots, j_k$  with the vertices in the bottom row of  $d_\beta$ . Then, we have that

$$F_\beta := \sum_{I, J} \gamma_{r_1, u_1} \gamma_{r_2, u_2} \cdots \gamma_{r_{\frac{l+k}{2}}, u_{\frac{l+k}{2}}} E_{I, J} \quad (22)$$

where the indices  $i_p, j_p$  range over  $1, 1', \dots, m, m'$ , where  $r_1, u_1, \dots, r_{\frac{l+k}{2}}, u_{\frac{l+k}{2}}$  is any permutation of the indices  $i_1, i_2, \dots, i_l, j_1, j_2, \dots, j_k$  such that the vertices corresponding to  $r_p, u_p$  are in the same block of  $\beta$ , and

$$\gamma_{r_p, u_p} := \begin{cases} \delta_{r_p, u_p} & \text{if the vertices corresponding to } r_p, u_p \text{ are in different rows of } d_\beta \\ \epsilon_{r_p, u_p} & \text{if the vertices corresponding to } r_p, u_p \text{ are in the same row of } d_\beta \end{cases} \quad (23)$$

Here,  $\epsilon_{r_p, u_p}$  is given by

$$\epsilon_{\alpha, \beta} = \epsilon_{\alpha', \beta'} = 0 \quad (24)$$

$$\epsilon_{\alpha,\beta'} = -\epsilon_{\alpha',\beta} = \delta_{\alpha,\beta} \quad (25)$$

In particular, the set

$$\{F_\beta \mid d_\beta \text{ is a } (k, l)\text{-Brauer diagram}\} \quad (26)$$

is a spanning set for  $\text{Hom}_{\text{Sp}(n)}((\mathbb{R}^n)^{\otimes k}, (\mathbb{R}^n)^{\otimes l})$ , for  $n = 2m$ , in the symplectic basis of  $\mathbb{R}^n$ , of size 0 when  $l + k$  is odd, and of size  $(l + k - 1)!!$  when  $l + k$  is even.

**Corollary 10 (Symplectic Group Equivariant Weight Matrices)** *For all non-negative integers  $l, k$  and positive even integers  $n$ , the weight matrix  $W$  that appears in an  $\text{Sp}(n)$ -equivariant linear layer function from  $(\mathbb{R}^n)^{\otimes k}$  to  $(\mathbb{R}^n)^{\otimes l}$  must be of the form*

$$W = \sum_{d_\beta \in B_k^l(n)} \lambda_\beta F_\beta \quad (27)$$

**Theorem 11 (Spanning set when  $G(n) = \text{SO}(n)$ )** *(Pearce-Crump, 2023a, Theorem 6.7)*

*For all non-negative integers  $l, k$  and positive even integers  $n$ , there is a surjection of vector spaces*

$$\Psi_{k,n}^l : D_k^l(n) \rightarrow \text{Hom}_{\text{SO}(n)}((\mathbb{R}^n)^{\otimes k}, (\mathbb{R}^n)^{\otimes l}) \quad (28)$$

that is given by

$$d_\beta \mapsto E_\beta \quad (29)$$

if  $d_\beta$  is a  $(k, l)$ -Brauer diagram, where  $E_\beta$  was defined in Theorem 7, and by

$$d_\alpha \mapsto H_\alpha \quad (30)$$

if  $d_\alpha$  is a  $(k + l) \setminus n$ -diagram, where  $H_\alpha$  is defined as follows.

Associate the indices  $i_1, i_2, \dots, i_l$  with the vertices in the top row of  $d_\alpha$ , and  $j_1, j_2, \dots, j_k$  with the vertices in the bottom row of  $d_\alpha$ . Suppose that there are  $s$  free vertices in the top row. Then there are  $n - s$  free vertices in the bottom row. Relabel the  $s$  free indices in the top row from left-to-right by  $t_1, \dots, t_s$ , and the  $n - s$  free indices in the bottom row from left-to-right by  $b_1, \dots, b_{n-s}$ . Then, we have that

$$H_\alpha := \sum_{I \in [n]^l, J \in [n]^k} \det(e_{T,B}) \delta(R, U) E_{I,J} \quad (31)$$

where  $\det(e_{T,B})$  is the determinant of the  $n \times n$  matrix

$$|e_{t_1} \ e_{t_2} \ \cdots \ e_{t_s} \ e_{b_1} \ \cdots \ e_{b_{n-s}}| \quad (32)$$

and

$$\delta(R, U) := \delta_{r_1, u_1} \delta_{r_2, u_2} \cdots \delta_{r_{\frac{l+k-n}{2}}, u_{\frac{l+k-n}{2}}} \quad (33)$$

Here,  $r_1, u_1, \dots, r_{\frac{l+k-n}{2}}, u_{\frac{l+k-n}{2}}$  is any permutation of the indices

$$\{i_1, \dots, i_l, j_1, \dots, j_k\} \setminus \{t_1, \dots, t_s, b_1, \dots, b_{n-s}\} \quad (34)$$

such that the vertices corresponding to  $r_p, u_p$  are in the same block of  $\alpha$ .



In particular, the set

$$\{E_\beta\}_\beta \cup \{H_\alpha\}_\alpha \quad (35)$$

where  $d_\beta$  is a  $(k, l)$ -Brauer diagram, and  $d_\alpha$  is a  $(l+k) \setminus n$ -diagram, is a spanning set for  $\text{Hom}_{SO(n)}((\mathbb{R}^n)^{\otimes k}, (\mathbb{R}^n)^{\otimes l})$  in the standard basis of  $\mathbb{R}^n$ .

**Corollary 12 (Special Orthogonal Group Equivariant Weight Matrices)** *For all non-negative integers  $l, k$  and positive integers  $n$ , the weight matrix  $W$  that appears in an  $SO(n)$ -equivariant linear layer function from  $(\mathbb{R}^n)^{\otimes k}$  to  $(\mathbb{R}^n)^{\otimes l}$  must be of the form*

$$W = \sum_{d_\beta \in D_k^l(n)} \lambda_\beta E_\beta + \sum_{d_\alpha \in D_k^l(n)} \lambda_\alpha H_\alpha \quad (36)$$

## 4 Equivariant Weight Matrices from Categories

In the previous section, we recalled the linear maps that can be used to obtain the equivariant weight matrices between tensor power spaces of  $\mathbb{R}^n$  for each of the four groups in question. To motivate the content of this section, we note that, for a given group  $G(n)$ , each of the weight matrices is in some sense similar, since they are determined in part by the layer spaces, which are tensor power representations that differ only in their order. Likewise, the vector spaces containing certain types of set partition diagrams are also, in some sense, similar, in that, for a fixed value of  $n$ , the vector spaces mostly differ by the values chosen for  $l$  and  $k$ , which represent the number of vertices in each row of a set partition diagram. We would like to formalise this intuition of similarity across different values of  $l$  and  $k$  for both the vector spaces of equivariant linear maps and the vector spaces containing certain types of set partition diagrams. For this, the concepts that appear in category theory are ideal, in that they are useful for abstracting away the specifics of structures in order to study their general properties. From the vector spaces that have similar properties, we create so-called monoidal categories, which are categories that have an additional operation for composing objects and morphisms, known as the tensor product, and then use them to create so-called monoidal functors, which are functors that preserve the tensor product between monoidal categories. We are particularly interested in the tensor product because the layer spaces are tensor power spaces of  $\mathbb{R}^n$ , and they differ only in the number of tensor products that are involved.

We wish to emphasise that we are not simply rewriting existing results in a different language, but that, as an outcome of this process, we obtain new insights into the equivariant neural networks for each group. In particular, we show that set partition diagrams that appear in monoidal categories have a string-like quality to them. By pulling on the strings or dragging their ends to different locations, we can use the monoidal functors to obtain new results that are relevant for the weight matrices that appear in these group equivariant neural networks. We summarise these new results at the end of this section.

### 4.1 Strict $\mathbb{R}$ -Linear Monoidal Categories and String Diagrams

We begin by introducing categories and functors that are **monoidal**. The monoidal property gives additional structure to the way in which objects and morphisms can be related. In particular, monoidal categories have an additional operation, known as a **bifunctor**, or a

**tensor product**, that enables objects and morphisms to be composed in a second way, relative to the usual definition of composition that exists in every category. We often call this additional composition **horizontal**, in contrast to the **vertical** composition that comes with any category. Crucially, monoidal functors preserve the tensor product across monoidal categories.

In this section, we assume knowledge of the definition of a category and the definition of a functor between categories. These definitions can be found in an introductory text on category theory, such as Leinster (2014); Mac Lane (1998) or Riehl (2017).

We assume throughout that all categories are **locally small**, which means that the collection of morphisms between any two objects is a set. In fact, all of the categories that we consider going forward have morphism sets that are vector spaces. Hence, the morphisms between objects are actually linear maps. For the definitions in this section, we follow the presentation that is given in Hu (2019) and Savage (2021).

**Definition 13** *A category  $\mathcal{C}$  is said to be **strict monoidal** if it comes with a functor  $\otimes : \mathcal{C} \times \mathcal{C} \rightarrow \mathcal{C}$ , known as a **bifunctor** or a **tensor product**, and a unit object  $\mathbb{1}$ , such that, for all objects  $X, Y, Z$  in  $\mathcal{C}$ , we have that*

$$(X \otimes Y) \otimes Z = X \otimes (Y \otimes Z) \tag{37}$$

$$(\mathbb{1} \otimes X) = X = (X \otimes \mathbb{1}) \tag{38}$$

and, for all morphisms  $f, g, h$  in  $\mathcal{C}$ , we have that

$$(f \otimes g) \otimes h = f \otimes (g \otimes h) \tag{39}$$

$$(1_{\mathbb{1}} \otimes f) = f = (f \otimes 1_{\mathbb{1}}) \tag{40}$$

where  $1_{\mathbb{1}}$  is the identity morphism  $\mathbb{1} \rightarrow \mathbb{1}$ . We often use the tuple  $(\mathcal{C}, \otimes_{\mathcal{C}}, \mathbb{1}_{\mathcal{C}})$  to refer to the strict monoidal category  $\mathcal{C}$ .

We have started with the definition of a *strict* monoidal category as opposed to that of a monoidal category since we can assume that all monoidal categories are strict, owing to a technical result known as Mac Lane’s Coherence Theorem. See Mac Lane (1998) for more details.

**Definition 14** *A category  $\mathcal{C}$  is said to be  **$\mathbb{R}$ -linear** if, for any two objects  $X, Y$  in  $\mathcal{C}$ , the morphism space  $\text{Hom}_{\mathcal{C}}(X, Y)$  is a vector space over  $\mathbb{R}$ , and the composition of morphisms is  $\mathbb{R}$ -bilinear.*

Combining Definitions 13 and 14, we get

**Definition 15** *A category  $\mathcal{C}$  is said to be **strict  $\mathbb{R}$ -linear monoidal** if it is a category that is both strict monoidal and  $\mathbb{R}$ -linear, such that the bifunctor  $\otimes$  is  $\mathbb{R}$ -bilinear.*

We now consider functors between strict  $\mathbb{R}$ -linear monoidal categories that preserve the tensor product.

**Definition 16** Suppose that  $(\mathcal{C}, \otimes_{\mathcal{C}}, \mathbf{1}_{\mathcal{C}})$  and  $(\mathcal{D}, \otimes_{\mathcal{D}}, \mathbf{1}_{\mathcal{D}})$  are two strict  $\mathbb{R}$ -linear monoidal categories.

A **strict  $\mathbb{R}$ -linear monoidal functor** from  $\mathcal{C}$  to  $\mathcal{D}$  is a functor  $\mathcal{F} : \mathcal{C} \rightarrow \mathcal{D}$  such that

1. for all objects  $X, Y$  in  $\mathcal{C}$ ,  $\mathcal{F}(X \otimes_{\mathcal{C}} Y) = \mathcal{F}(X) \otimes_{\mathcal{D}} \mathcal{F}(Y)$
2. for all morphisms  $f, g$  in  $\mathcal{C}$ ,  $\mathcal{F}(f \otimes_{\mathcal{C}} g) = \mathcal{F}(f) \otimes_{\mathcal{D}} \mathcal{F}(g)$
3.  $\mathcal{F}(\mathbf{1}_{\mathcal{C}}) = \mathbf{1}_{\mathcal{D}}$ , and
4. for all objects  $X, Y$  in  $\mathcal{C}$ , the map

$$\mathrm{Hom}_{\mathcal{C}}(X, Y) \rightarrow \mathrm{Hom}_{\mathcal{D}}(\mathcal{F}(X), \mathcal{F}(Y)) \quad (41)$$

given by  $f \mapsto \mathcal{F}(f)$  is  $\mathbb{R}$ -linear.

Strict monoidal categories are particularly interesting because they can be represented by a very useful diagrammatic language known as **string diagrams**. We will see that, as this language is, in some sense, geometric in nature, it is much easier to work with these diagrams compared with their equivalent algebraic form.

**Definition 17 (String Diagrams)** Suppose that  $\mathcal{C}$  is a strict monoidal category. Let  $W, X, Y$  and  $Z$  be objects in  $\mathcal{C}$ , and let  $f : X \rightarrow Y$ ,  $g : Y \rightarrow Z$ , and  $h : W \rightarrow Z$  be morphisms in  $\mathcal{C}$ . Then we can represent the morphisms  $1_X : X \rightarrow X$ ,  $f : X \rightarrow Y$ ,  $g \circ f : X \rightarrow Z$  and  $f \otimes h : X \otimes W \rightarrow Y \otimes Z$  as string diagrams in the following way:

$$\quad (42)$$

In particular, the vertical composition of morphisms  $g \circ f$  is obtained by placing  $g$  above  $f$ , and the horizontal composition of morphisms  $f \otimes h$  is obtained by horizontally placing  $f$  to the left of  $h$ .

We will often omit the labelling of the objects when they are clear or when they are not important.

As an example of how useful string diagrams are when working with strict monoidal categories, the associativity of the bifunctor given in (39) becomes immediately apparent. Another, more involved, example is given by the interchange law that exists for any strict monoidal category. It can be expressed algebraically as

$$(\mathbf{1} \otimes g) \circ (f \otimes \mathbf{1}) = f \otimes g = (f \otimes \mathbf{1}) \circ (\mathbf{1} \otimes g) \quad (43)$$

Without string diagrams, it is somewhat tedious to prove this result. Indeed, for the left hand equality of (43), we have that

$$(\mathbf{1} \otimes g) \circ (f \otimes \mathbf{1}) = (\otimes(\mathbf{1}, g)) \circ (\otimes(f, \mathbf{1})) = \otimes((\mathbf{1}, g) \circ (f, \mathbf{1})) = \otimes((f, g)) = f \otimes g \quad (44)$$

where we have used the definition of composition in  $\mathcal{C} \times \mathcal{C}$  and the fact that  $\otimes : \mathcal{C} \times \mathcal{C} \rightarrow \mathcal{C}$  is a functor. A similar calculation also holds for the right hand equality of (43).

However, with string diagram, the result is intuitively obvious, if we allow ourselves to deform the diagrams by pulling on the strings:

$$(45)$$

## 4.2 Categorification

Previously, we defined a vector space for each non-negative integer  $l$  and  $k$  that is the  $\mathbb{R}$ -linear span of a certain subset of  $(k, l)$ -partition diagrams. However, it is clear that, for all values of  $l$  and  $k$ , these vector spaces are all similar in nature, in that the set partition diagrams only differ by the number of vertices that appear in each row and by the connections that are made between vertices. Moreover, set partition diagrams look like string diagrams. Given that string diagrams represent strict monoidal categories, and that we have a collection of vector spaces for certain subsets of set partition diagrams, this implies that we should have a number of strict  $\mathbb{R}$ -linear monoidal categories. We formalise this intuition below.

### 4.2.1 PARTITION CATEGORIES

We assume throughout that  $l$  and  $k$  are non-negative integers and that  $n$  is a positive integer. In Section 3.2, we defined the partition vector space  $P_k^l(n)$ , which has a basis consisting of all possible  $(k, l)$ -partition diagrams. In order to obtain a category from these vector spaces, we need to define the following two  $\mathbb{R}$ -bilinear operations on  $(k, l)$ -partition diagrams:

$$\text{composition: } \bullet : P_l^m(n) \times P_k^l(n) \rightarrow P_k^m(n) \quad (46)$$

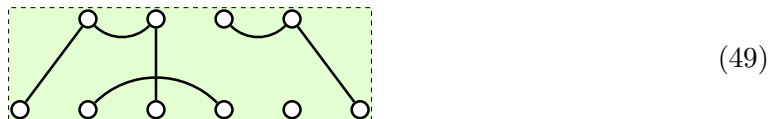
$$\text{tensor product: } \otimes : P_k^l(n) \times P_q^m(n) \rightarrow P_{k+q}^{l+m}(n) \quad (47)$$

They are given as follows:

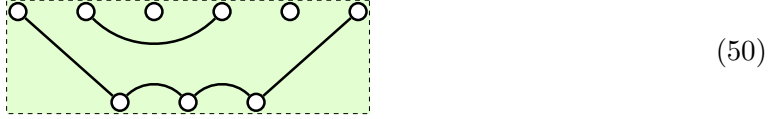
**Definition 18 (Composition)** *Let  $d_{\pi_1} \in P_k^l(n)$  and  $d_{\pi_2} \in P_l^m(n)$ . First, we concatenate the diagrams, written  $d_{\pi_2} \circ d_{\pi_1}$ , by putting  $d_{\pi_1}$  below  $d_{\pi_2}$ , concatenating the edges in the middle row of vertices, and then removing all connected components that lie entirely in the middle row of the concatenated diagrams. Let  $c(d_{\pi_2}, d_{\pi_1})$  be the number of connected components that are removed from the middle row in  $d_{\pi_2} \circ d_{\pi_1}$ . Then the composition is defined, using infix notation, as*

$$d_{\pi_2} \bullet d_{\pi_1} := n^{c(d_{\pi_2}, d_{\pi_1})} (d_{\pi_2} \circ d_{\pi_1}) \quad (48)$$

**Example 4** *If  $d_{\pi_2}$  is the  $(6, 4)$ -partition diagram*



and  $d_{\pi_1}$  is the  $(3, 6)$ -partition diagram



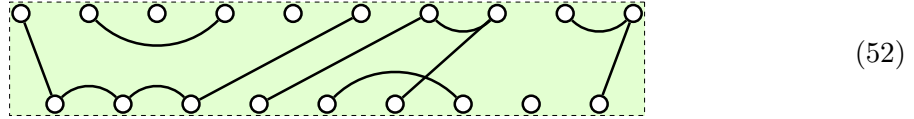
then we have that  $d_{\pi_2} \circ d_{\pi_1}$  is the  $(3, 4)$ -partition diagram



and so  $d_{\pi_2} \bullet d_{\pi_1}$  is the diagram (51) multiplied by  $n^2$ , since two connected components were removed from the middle row of  $d_{\pi_2} \circ d_{\pi_1}$ .

**Definition 19 (Tensor Product)** Let  $d_{\pi_1} \in P_k^l(n)$  and  $d_{\pi_2} \in P_q^m(n)$ . Then  $d_{\pi_1} \otimes d_{\pi_2}$  is defined to be the  $(k + q, l + m)$ -partition diagram that is obtained by horizontally placing  $d_{\pi_1}$  to the left of  $d_{\pi_2}$  without any overlapping of vertices.

**Example 5** The tensor product  $d_{\pi_1} \otimes d_{\pi_2}$ , for  $d_{\pi_1}$  and  $d_{\pi_2}$  given in Example 4, is the  $(9, 10)$ -partition diagram



It is clear that both the composition and the tensor product operations are associative. Consequently, we have the following category:

**Definition 20** We define the **partition category**  $\mathcal{P}(n)$  to be the category whose objects are the non-negative integers, and, for any pair of objects  $k$  and  $l$ , the morphism space  $\text{Hom}_{\mathcal{P}(n)}(k, l)$  is  $P_k^l(n)$ .

The vertical composition of morphisms is the composition of partition diagrams given in Definition 18; the horizontal composition of morphisms is the tensor product of partition diagrams given in Definition 19; and the unit object is 0.

For  $B_k^l(n)$ , we can inherit the composition and tensor product operations from the composition and tensor product operations for  $P_k^l(n)$ , giving the following category:

**Definition 21** We define the **Brauer category**  $\mathcal{B}(n)$  to be the category whose objects are the same as those of  $\mathcal{P}(n)$  and, for any pair of objects  $k$  and  $l$ , the morphism space  $\text{Hom}_{\mathcal{B}(n)}(k, l)$  is  $B_k^l(n)$ .

The vertical and horizontal composition of morphisms and the unit object are the same as those defined for  $\mathcal{P}(n)$ .

We claim the following result.

**Proposition 22** *The partition category  $\mathcal{P}(n)$  and the Brauer category  $\mathcal{B}(n)$  are strict  $\mathbb{R}$ -linear monoidal categories.*

**Proof.** We prove this result for the partition category since the proof for the Brauer category is effectively the same.

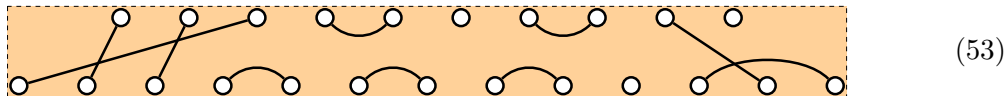
$\mathcal{P}(n)$  is a strict monoidal category because the bifunctor on objects reduces to the addition of natural numbers, which is associative and the bifunctor on morphisms is the tensor product of linear combinations of partition diagrams that is given in Definition 18, which is associative by definition.

$\mathcal{P}(n)$  is  $\mathbb{R}$ -linear because the morphism space between any two objects is by definition a vector space, and the composition of morphisms is  $\mathbb{R}$ -bilinear by definition. For the same reason, the bifunctor is also  $\mathbb{R}$ -bilinear. ■

We can also obtain a strict  $\mathbb{R}$ -linear monoidal category  $\mathcal{BG}(n)$  from the Brauer–Grood vector spaces  $D_k^l(n)$ . We will call  $\mathcal{BG}(n)$  the **Brauer–Grood category**, although it sometimes appears in the literature under different names, such as the Jellyfish Brauer category in Comes (2020). Showing that  $\mathcal{BG}(n)$  is strict  $\mathbb{R}$ -linear monoidal is a long and arduous computation that has previously appeared in Lehrer and Zhang (2012, 2018) – namely, it is the result of combining the proof of Lehrer and Zhang (2012, Theorem 2.6) together with the proof of Lehrer and Zhang (2018, Theorem 6.1). Hence, for brevity, we omit it here.

Instead, we show only part of the definition of the horizontal composition, since it will be used in Section 5. To define the horizontal composition in full, we would need to define it on four possible cases of ordered pairs of diagrams. One of those ordered pairs is  $(d_\beta, d_\alpha)$ , where  $d_\beta$  is a  $(k, l)$ -Brauer diagram and  $d_\alpha$  is an  $(m + q) \setminus n$ -diagram. In this case, the horizontal composition gives the  $(l + m + k + q) \setminus n$ -diagram that is obtained by horizontally placing  $d_\beta$  to the left of  $d_\alpha$  without any overlapping of vertices.

**Example 6** *Recalling the  $(7, 5)$ -Brauer diagram  $d_\beta$  and the  $(5 + 6) \setminus 3$ -diagram  $d_\alpha$  that was given in Example 3, we see that  $d_\beta \otimes d_\alpha$  is the  $(10 + 13) \setminus 3$ -diagram*



For the sake of completeness, we provide the framework of the definition of the Brauer–Grood category below.

**Definition 23** *The **Brauer–Grood category**  $\mathcal{BG}(n)$  is the category whose objects are the same as those of  $\mathcal{P}(n)$  and, for any pair of objects  $k$  and  $l$ , the morphism space  $\text{Hom}_{\mathcal{BG}(n)}(k, l)$  is  $D_k^l(n)$ . [We have omitted the full definition of the vertical composition of morphisms and the horizontal composition of morphisms.] The unit object is 0.*

We will refer to these categories in general as **partition categories**. When we wish to specifically reference the partition category  $\mathcal{P}(n)$ , we will explicitly write  $\mathcal{P}(n)$  to clarify that we mean this particular category.

### 4.2.2 GROUP REPRESENTATION CATEGORIES

It is not just the partition vector spaces that are similar for different values of  $l$  and  $k$ . The tensor power spaces of  $\mathbb{R}^n$  that make up the layer spaces and, in particular, the equivariant linear maps between them, are also similar for different values of  $l$  and  $k$ . To form a category from these representations and the linear maps between them, we first need to define a category for all representations of a group.

**Definition 24** *Let  $G$  be a group. Then  $\text{Rep}(G)$  is the category whose objects are pairs  $(V, \rho_V)$ , where  $\rho_V : G \rightarrow GL(V)$  is a representation of  $G$ , and, for any pair of objects  $(V, \rho_V)$  and  $(W, \rho_W)$ , the morphism space,  $\text{Hom}_{\text{Rep}(G)}((V, \rho_V), (W, \rho_W))$ , is precisely the vector space of  $G$ -equivariant linear maps  $V \rightarrow W$ ,  $\text{Hom}_G(V, W)$ .*

*The vertical composition of morphisms is given by the composition of linear maps, the horizontal composition of morphisms is given by the tensor product of linear maps, both of which are associative operations, and the unit object is given by  $(\mathbb{R}, 1_{\mathbb{R}})$ , where  $1_{\mathbb{R}}$  is the one-dimensional trivial representation of  $G$ .*

If  $G = G(n)$  is a subgroup of  $GL(n)$  (and, in particular, one of  $S_n, O(n), SO(n)$  or  $Sp(n)$ ), then we have the following category.

**Definition 25** *If  $G(n)$  is a subgroup of  $GL(n)$ , then the **tensor power representation category**  $\mathcal{C}(G(n))$  is the category whose objects are pairs  $\{((\mathbb{R}^n)^{\otimes k}, \rho_k)\}_{k \in \mathbb{Z}_{\geq 0}}$ , where  $\rho_k : G(n) \rightarrow GL((\mathbb{R}^n)^{\otimes k})$  is the representation of  $G(n)$  given in Section 3.1, and, for any pair of objects  $((\mathbb{R}^n)^{\otimes k}, \rho_k)$  and  $((\mathbb{R}^n)^{\otimes l}, \rho_l)$ , the morphism space is precisely  $\text{Hom}_{G(n)}((\mathbb{R}^n)^{\otimes k}, (\mathbb{R}^n)^{\otimes l})$ .*

*The vertical and horizontal composition of morphisms together with the unit object are inherited from  $\text{Rep}(G(n))$ .*

**Proposition 26** *For any subgroup  $G(n)$  of  $GL(n)$ ,  $\mathcal{C}(G(n))$  is a full subcategory of the category of representations of  $G(n)$ ,  $\text{Rep}(G(n))$ ; that is, for every pair of objects in  $\mathcal{C}(G(n))$ , every morphism between them in  $\text{Rep}(G(n))$  is a morphism in  $\mathcal{C}(G(n))$ . In particular,  $\mathcal{C}(G(n))$  is a strict  $\mathbb{R}$ -linear monoidal category.*

**Proof.** It is clear from the definitions that  $\mathcal{C}(G(n))$  is a subcategory of  $\text{Rep}(G(n))$ .  $\mathcal{C}(G(n))$  is a full subcategory of  $\text{Rep}(G(n))$ , as, for any pair of objects  $((\mathbb{R}^n)^{\otimes k}, \rho_k)$  and  $((\mathbb{R}^n)^{\otimes l}, \rho_l)$  in  $\mathcal{C}(G(n))$ , the morphism space in  $\mathcal{C}(G(n))$  is the same as the one in  $\text{Rep}(G(n))$ .

$\mathcal{C}(G(n))$  can immediately be seen to be a strict monoidal category because the bifunctor on objects is the tensor product of vector spaces, which is associative, and the bifunctor on morphisms is the tensor product on linear maps between vector spaces, which is also associative.

$\mathcal{C}(G(n))$  is  $\mathbb{R}$ -linear because the morphism space for any two objects is a vector space over  $\mathbb{R}$  and the composition of morphisms is  $\mathbb{R}$ -bilinear because composition is  $\mathbb{R}$ -bilinear for linear maps on vector spaces. It is also clear that the bifunctor  $\otimes$  is  $\mathbb{R}$ -bilinear since it is the standard tensor product for vector spaces. ■

### 4.3 Monoidal Functors from Partition Categories to Group Representation Categories

In Section 3.3, we reviewed a number of linear maps between certain partition vector spaces and the vector space of equivariant linear maps between tensor power representations for four subgroups  $G(n)$  of  $GL(n)$ . We now show that these linear maps are the result of something stronger, namely that they are the linear maps that come from the existence of a strict  $\mathbb{R}$ -linear monoidal functor between a partition category and its associated tensor power representation category. In each of the following four theorems, we state that the functors are **full**; that is, the underlying map between morphism spaces, having chosen a pair of objects in the domain category, is surjective.

**Theorem 27** *There exists a full, strict  $\mathbb{R}$ -linear monoidal functor*

$$\Theta : \mathcal{P}(n) \rightarrow \mathcal{C}(S_n) \quad (54)$$

that is defined on the objects of  $\mathcal{P}(n)$  by  $\Theta(k) := ((\mathbb{R}^n)^{\otimes k}, \rho_k)$  and, for any objects  $k, l$  of  $\mathcal{P}(n)$ , the map

$$\mathrm{Hom}_{\mathcal{P}(n)}(k, l) \rightarrow \mathrm{Hom}_{\mathcal{C}(S_n)}(\Theta(k), \Theta(l)) \quad (55)$$

is precisely the map

$$\Theta_{k,n}^l : P_k^l(n) \rightarrow \mathrm{Hom}_{S_n}((\mathbb{R}^n)^{\otimes k}, (\mathbb{R}^n)^{\otimes l}) \quad (56)$$

given in Theorem 5.

**Theorem 28** *There exists a full, strict  $\mathbb{R}$ -linear monoidal functor*

$$\Phi : \mathcal{B}(n) \rightarrow \mathcal{C}(O(n)) \quad (57)$$

that is defined on the objects of  $\mathcal{B}(n)$  by  $\Phi(k) := ((\mathbb{R}^n)^{\otimes k}, \rho_k)$  and, for any objects  $k, l$  of  $\mathcal{B}(n)$ , the map

$$\mathrm{Hom}_{\mathcal{B}(n)}(k, l) \rightarrow \mathrm{Hom}_{\mathcal{C}(O(n))}(\Phi(k), \Phi(l)) \quad (58)$$

is the map

$$\Phi_{k,n}^l : B_k^l(n) \rightarrow \mathrm{Hom}_{O(n)}((\mathbb{R}^n)^{\otimes k}, (\mathbb{R}^n)^{\otimes l}) \quad (59)$$

given in Theorem 7.

**Theorem 29** *There exists a full, strict  $\mathbb{R}$ -linear monoidal functor*

$$X : \mathcal{B}(n) \rightarrow \mathcal{C}(Sp(n)) \quad (60)$$

that is defined on the objects of  $\mathcal{B}(n)$  by  $X(k) := ((\mathbb{R}^n)^{\otimes k}, \rho_k)$  and, for any objects  $k, l$  of  $\mathcal{B}(n)$ , the map

$$\mathrm{Hom}_{\mathcal{B}(n)}(k, l) \rightarrow \mathrm{Hom}_{\mathcal{C}(Sp(n))}(\Phi(k), \Phi(l)) \quad (61)$$

is the map

$$X_{k,n}^l : B_k^l(n) \rightarrow \mathrm{Hom}_{Sp(n)}((\mathbb{R}^n)^{\otimes k}, (\mathbb{R}^n)^{\otimes l}) \quad (62)$$

given in Theorem 9.



**Theorem 30** *There exists a full, strict  $\mathbb{R}$ -linear monoidal functor*

$$\Psi : \mathcal{BG}(n) \rightarrow \mathcal{C}(SO(n)) \quad (63)$$

that is defined on the objects of  $\mathcal{BG}(n)$  by  $\Psi(k) := ((\mathbb{R}^n)^{\otimes k}, \rho_k)$  and, for any objects  $k, l$  of  $\mathcal{B}(n)$ , the map

$$\mathrm{Hom}_{\mathcal{BG}(n)}(k, l) \rightarrow \mathrm{Hom}_{\mathcal{C}(SO(n))}(\Phi(k), \Phi(l)) \quad (64)$$

is the map

$$\Psi_{k,n}^l : D_k^l(n) \rightarrow \mathrm{Hom}_{SO(n)}((\mathbb{R}^n)^{\otimes k}, (\mathbb{R}^n)^{\otimes l}) \quad (65)$$

given in Theorem 11.

We only show the proof of Theorem 27 in full since the proofs of Theorems 28 and 29 are almost identical. The proof of Theorem 30 can be found in Lehrer and Zhang (2018, Theorem 6.1).

**Proof.** [Proof of Theorem 27] We prove this theorem in a series of steps.

**Step 1:** We need to show that  $\Theta : \mathcal{P}(n) \rightarrow \mathcal{C}(S_n)$  is a functor.

We prove this step in three parts.

- $\Theta$  maps the objects of  $\mathcal{P}(n)$  to the objects of  $\mathcal{C}(S_n)$  by definition.
- It is enough to show that  $\Theta(g)\Theta(f) = \Theta(g \bullet f)$  on arbitrary basis elements of arbitrary morphism spaces where the codomain of  $f$  is the domain of  $g$  because the morphism spaces are vector spaces.

Let  $f = d_{\pi_1}$  be a  $(k, l)$ -partition diagram, and let  $g = d_{\pi_2}$  be a  $(l, m)$ -partition diagram. Then, by Definition 18, we have that

$$d_{\pi_2} \bullet d_{\pi_1} = n^{c(d_{\pi_2}, d_{\pi_1})} d_{\pi_3} \quad (66)$$

where  $d_{\pi_3}$  be the composition  $d_{\pi_2} \circ d_{\pi_1}$  expressed as a  $(k, m)$ -partition diagram. Then

$$\Theta(g \bullet f) = \Theta(d_{\pi_2} \bullet d_{\pi_1}) = n^{c(d_{\pi_2}, d_{\pi_1})} D_{\pi_3} \quad (67)$$

We also have that

$$\Theta(g)\Theta(f) = D_{\pi_2} D_{\pi_1} = \left( \sum_{I \in [n]^m, K \in [n]^l} \delta_{\pi_2, (I, K)} E_{I, K} \right) \left( \sum_{L \in [n]^l, J \in [n]^k} \delta_{\pi_1, (L, J)} E_{L, J} \right) \quad (68)$$

$$= \sum_{I \in [n]^m, K \in [n]^l, J \in [n]^k} \delta_{\pi_2, (I, K)} \delta_{\pi_1, (K, J)} E_{I, K} E_{K, J} \quad (69)$$

For fixed  $I, J$ , consider

$$\sum_{K \in [n]^l} \delta_{\pi_2, (I, K)} \delta_{\pi_1, (K, J)} \quad (70)$$

This is equal to

$$n^{c(d_{\pi_2}, d_{\pi_1})} \delta_{\pi_3, (I, J)} \quad (71)$$

Indeed, for fixed  $I, J$ ,  $\delta_{\pi_3, (I, J)}$  is 1 if and only if both  $\delta_{\pi_2, (I, K)}$  and  $\delta_{\pi_1, (K, J)}$  are 1 for some  $K \in [n]^l$  since  $d_{\pi_3}$  is the composition  $d_{\pi_2} \circ d_{\pi_1}$ . The number of such  $K$  is determined only by the vertices that appear in connected components that are removed from the middle row of  $d_{\pi_2} \circ d_{\pi_1}$ , since, for fixed  $I, J$ , only these vertices can be freely chosen if we want both  $\delta_{\pi_2, (I, K)}$  and  $\delta_{\pi_1, (K, J)}$  to be 1. However, since the entries in each connected component must be the same for both  $\delta_{\pi_2, (I, K)}$  and  $\delta_{\pi_1, (K, J)}$  to be 1, this implies that the number of  $K \in [n]^l$  such that both  $\delta_{\pi_2, (I, K)}$  and  $\delta_{\pi_1, (K, J)}$  are 1 is  $n^{c(d_{\pi_2}, d_{\pi_1})}$ .

Hence (69) becomes

$$\sum_{I \in [n]^m, J \in [n]^k} n^{c(d_{\pi_2}, d_{\pi_1})} \delta_{\pi_3, (I, J)} E_{I, J} = n^{c(d_{\pi_2}, d_{\pi_1})} E_{\pi_3} \quad (72)$$

and so, by (67), we have that  $\Theta(g)\Theta(f) = \Theta(g \bullet f)$ , as required.

- For each object  $k$  in  $\mathcal{P}(n)$ , the identity morphism  $1_k$  is the  $(k, k)$ -partition diagram  $d_\pi$  where  $\pi$  is the set partition

$$\{1, k+1 \mid 2, k+2 \mid \cdots \mid k, 2k\} \quad (73)$$

of  $[2k]$ , and its image under  $d_\pi \mapsto D_\pi$  is the  $n^k \times n^k$  identity matrix, as required.

**Step 2:** We need to show that  $\Theta : \mathcal{P}(n) \rightarrow \mathcal{C}(S_n)$  is full.

The functor  $\Theta$  is full because, for all objects  $k, l$  in  $\mathcal{P}(n)$ , the map (55) is (56), by definition, and this map is surjective by Theorem 5.

**Step 3:** We need to show that  $\Theta : \mathcal{P}(n) \rightarrow \mathcal{C}(S_n)$  is strict  $\mathbb{R}$ -linear monoidal.

To show that  $\Theta$  is strict  $\mathbb{R}$ -linear monoidal, we need to show that  $\Theta$  satisfies the conditions given in Definition 16. The picture to have in mind for point 2 below is that the tensor product on set partition diagrams places the diagrams side-by-side, without any overlapping of vertices.

1. Let  $k, l$  be any two objects in  $\mathcal{P}(n)$ . Then

$$\Theta(k \otimes l) = \Theta(k + l) \quad (74)$$

$$= ((\mathbb{R}^n)^{\otimes k+l}, \rho_{k+l}) \quad (75)$$

$$= ((\mathbb{R}^n)^{\otimes k} \otimes (\mathbb{R}^n)^{\otimes l}, \rho_k \otimes \rho_l) \quad (76)$$

$$= \Theta(k) \otimes \Theta(l) \quad (77)$$

2. It is enough to prove this condition on arbitrary basis elements of arbitrary morphism spaces as the morphism spaces are vector spaces. Suppose that  $f : k \rightarrow l$  and  $g :$

$q \rightarrow m$  are two basis elements in  $\text{Hom}_{\mathcal{P}(n)}(k, l)$  and  $\text{Hom}_{\mathcal{P}(n)}(q, m)$  respectively. Then  $f = d_\pi$  for some set partition  $\pi$  of  $[l + k]$ , and  $g = d_\tau$  for some set partition  $\tau$  of  $[m + q]$ .

As  $\text{Hom}_{\mathcal{P}(n)}(k, l) = P_k^l(n)$  and  $\text{Hom}_{\mathcal{P}(n)}(q, m) = P_q^m(n)$ , we have, by Definition 19, that  $f \otimes g$  is an element of  $P_{k+q}^{l+m}(n) = \text{Hom}_{\mathcal{P}(n)}(k + q, l + m)$ .

In particular,  $f \otimes g = d_\omega$  for the set partition  $\omega := \pi \cup \tau$  of  $[l + m + k + q]$ .

By Theorem 5, we have that  $\Theta(f) = D_\pi$ ,  $\Theta(g) = D_\tau$ , and  $\Theta(f \otimes g) = D_\omega$ .

We now show that  $\Theta(f) \otimes \Theta(g) = \Theta(f \otimes g)$ . Indeed, we have that

$$\Theta(f) \otimes \Theta(g) = D_\pi \otimes D_\tau \tag{78}$$

$$= \left( \sum_{I \in [n]^l, J \in [n]^k} \delta_{\pi, (I, J)} E_{I, J} \right) \otimes \left( \sum_{X \in [n]^m, Y \in [n]^q} \delta_{\tau, (X, Y)} E_{X, Y} \right) \tag{79}$$

$$= \sum_{(I, X) \in [n]^{l+m}, (J, Y) \in [n]^{k+q}} \delta_{\omega, (I, X), (J, Y)} E_{(I, X), (J, Y)} \tag{80}$$

$$= D_\omega \tag{81}$$

$$= \Theta(f \otimes g) \tag{82}$$

where (80) holds because  $S_\pi((I, J)) \cup S_\tau((X, Y)) = S_\omega((I, X), (J, Y))$ .

3. It is clear from the statement of the theorem that  $\Theta$  sends the unit object  $0$  in  $\mathcal{P}(n)$  to  $(\mathbb{R}, 1_{\mathbb{R}})$ , which is the unit object in  $\mathcal{C}(S_n)$ .
4. This is immediate because the map (56) is  $\mathbb{R}$ -linear by Theorem 5. ■

#### 4.4 Implications for Group Equivariant Neural Networks

The theorems in Section 4.3 imply several key statements that are crucial for the group equivariant neural networks under consideration. These statements can be formulated as follows.

1. To understand and work with any matrix in  $\text{Hom}_{G(n)}((\mathbb{R}^n)^{\otimes k}, (\mathbb{R}^n)^{\otimes l})$ , it is enough to work with the subset of  $(k, l)$ -partition diagrams that correspond to  $G(n)$ . This is because we can express any matrix in terms of the set of spanning set elements for  $\text{Hom}_{G(n)}((\mathbb{R}^n)^{\otimes k}, (\mathbb{R}^n)^{\otimes l})$ , and these correspond bijectively with the subset of  $(k, l)$ -partition diagrams that corresponds to  $G(n)$ . We can recover the matrix itself by applying the appropriate monoidal functor to the set partition diagrams because the monoidal functors are full.
2. We can manipulate the connected components and vertices of  $(k, l)$ -partition diagrams to obtain new set partition diagrams. Indeed, as the partition categories are strict monoidal, this means that the  $(k, l)$ -partition diagrams in a partition category are string diagrams. Statement 1 immediately implies that we will obtain new matrices between tensor power spaces of  $\mathbb{R}^n$  that are equivariant to  $G(n)$  from the resulting set partition diagrams.

3. If a  $(k, l)$ -partition diagram can be decomposed as a tensor product of smaller set partition diagrams, then the corresponding matrix can also be decomposed as a tensor product of smaller sized matrices, each of which is equivariant to  $G(n)$ . This is because the functors are monoidal.

In the following section, we present our main contribution. We use the monoidal functors that we have established for each of the four groups, together with the implications for the group equivariant neural networks given above, to construct a fast multiplication algorithm for passing a vector through a linear layer function that appears in such a network.

## 5 Algorithm for Computing with Equivariant Weight Matrices

Suppose that we would like to pass a vector  $v \in (\mathbb{R}^n)^{\otimes k}$  through a linear layer function that lives in  $\text{Hom}_{G(n)}((\mathbb{R}^n)^{\otimes k}, (\mathbb{R}^n)^{\otimes l})$ . A naive implementation of the matrix multiplication between the weight matrix and the vector has a time complexity equal to  $O(n^{l+k})$ . We show that we can construct a fast multiplication algorithm that reduces the time complexity exponentially for each of the groups  $G(n)$  in question.

It is important to highlight that, since we have at least a spanning set of the vector space  $\text{Hom}_{G(n)}((\mathbb{R}^n)^{\otimes k}, (\mathbb{R}^n)^{\otimes l})$  for each group  $G(n)$  that appeared in the previous chapter, it is enough to describe an algorithm for how to multiply  $v$  by a spanning set element since we can extend the result by linearity. This linearity provides an extra advantage in that it enables the fast matrix multiplication of an input vector  $v \in (\mathbb{R}^n)^{\otimes k}$  with a weight matrix in  $\text{Hom}_{G(n)}((\mathbb{R}^n)^{\otimes k}, (\mathbb{R}^n)^{\otimes l})$  to be executed in parallel, namely by performing the fast matrix multiplication on each of the spanning set elements that make up the weight matrix.

We begin by introducing a new class of set partition diagrams that we have termed **algorithmically planar**.

### 5.1 Algorithmically Planar Set Partition Diagrams

Recall that each spanning set element in  $\text{Hom}_{G(n)}((\mathbb{R}^n)^{\otimes k}, (\mathbb{R}^n)^{\otimes l})$  corresponds to a set partition diagram under a monoidal functor for  $G(n)$ , and that a set partition diagram is a string diagram since it is a morphism in a monoidal category. This leads to the following question that we use as motivation: can we use the string-like property of each set partition diagram to gain control over how the matrix multiplication operation is performed between the spanning set element and the vector?

There are a few guiding principles that we use to construct the algorithm.

Ideally, we would like to break the matrix multiplication operation down into a series of computations, each of which is indecomposable. Given the monoidal functor relationships between set partition diagrams and matrix operations, we know that the smallest possible computations that are available to us correspond precisely with the smallest indecomposable set partition diagrams. In general, set partition diagrams that consist only of one block are the smallest indecomposable diagrams. The exception is for  $(l+k)\setminus n$ -diagrams, where the smallest indecomposable diagrams are either those consisting of a single block of two vertices or a diagram consisting of all of the free vertices taken together. Moreover, a single block can live either entirely in the top row, entirely in the bottom row, or in both rows. Hence,

we see that there are only a few classes of indecomposable diagrams that are smallest. As a result, there are only a few classes of indecomposable matrix operations that are smallest.

We can say more. Since the matrices that we obtain must come from set partition diagrams, the most efficient matrices that we can construct are a Kronecker product of indecomposable matrices. But also, since indecomposable matrices come from indecomposable set partition diagrams, this implies that the most efficient matrices that we can construct come from set partition diagrams that decompose into a tensor product of the smallest indecomposable set partition diagrams. Moreover, we would like to choose the order in which the indecomposable matrices appear in the Kronecker product because each indecomposable matrix performs a certain operation and we would like them to be executed in an order that is as efficient as possible. For example, it is best to zero out as many terms as possible in the input vector first, if such an operation can be performed, since this reduces the number of elements that need to be operated on going forward. After this, it is better to perform tensor contraction operations before performing copying operations, because this reduces the number of elements that need to be copied. It is clear that choosing any other order for these operations would make the overall algorithm less efficient. We will see that each of these operations can be understood easily in their equivalent diagram form.

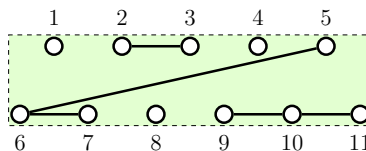
Consequently, from the set partition diagram that corresponds to the spanning set element, we would like to create another set partition diagram that decomposes into a tensor product of the smallest possible indecomposable set partition diagrams and are ordered such that the indecomposable matrix operations that appear in the corresponding Kronecker product will be performed most efficiently.

We call these special set partition diagrams algorithmically planar, and by construction they are the most efficient diagrams for performing matrix multiplication. They are defined as follows.

**Definition 31** *A  $(k, l)$ -partition diagram is said to be **algorithmically planar** if it satisfies the following conditions:*

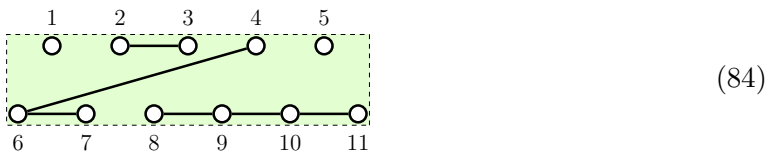
- *The connected components that are solely in the bottom row are lined up sequentially, starting from the far right hand side, such that the vertices in each connected component are in consecutive order. We also require that these connected components are ordered by their size, starting on the far right hand side with the largest and decreasing in size as we move towards the left, for reasons that will become clear when we conduct a time complexity analysis of the multiplication algorithm for the symmetric group.*
- *The connected components that are solely in the top row are lined up sequentially, starting from the far left hand side, such that the vertices in each connected component are in consecutive order. (Note that these connected components can be in any order.)*
- *The connected components between different rows are such that no two subsets cross.*

**Example 7** *The  $(6, 5)$ -partition diagram*

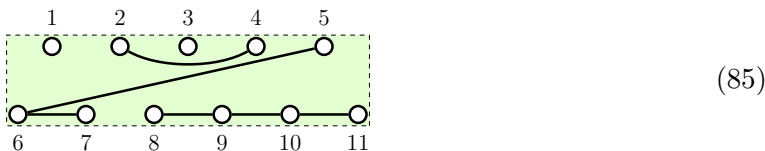


(83)

is algorithmically planar. However, the  $(6, 5)$ -partition diagram



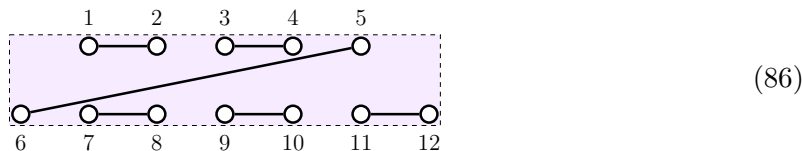
is not algorithmically planar because the connected component consisting solely of vertex 5 is not adjacent to a connected component that lives solely in the top row, and the  $(6, 5)$ -partition diagram



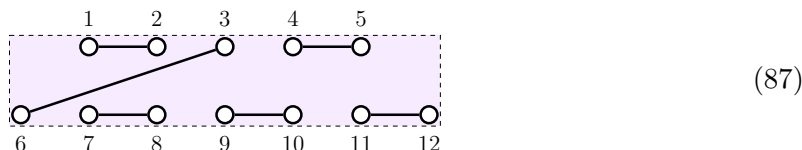
is also not algorithmically planar because the vertices in the connected component  $\{2, 4\}$  are not in consecutive order.

**Definition 32** A  $(k, l)$ -Brauer diagram is said to be **algorithmically planar** if it is an algorithmically planar  $(k, l)$ -partition diagram that is also a Brauer diagram.

**Example 8** The  $(7, 5)$ -Brauer diagram



is algorithmically planar, whereas the  $(7, 5)$ -Brauer diagram



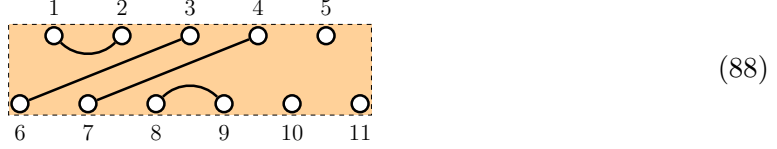
is not algorithmically planar.

**Definition 33** An  $(l + k) \setminus n$ -diagram is said to be **algorithmically planar** if it satisfies the following conditions:

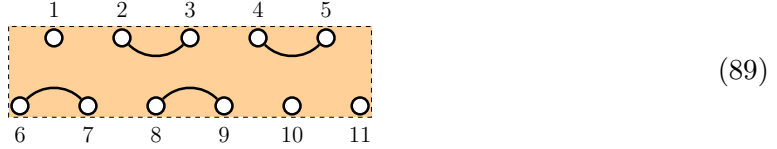
- The free vertices in the bottom row start from the far right hand side and are lined up sequentially.
- The free vertices in the top row also start from the far right hand side and are lined up sequentially.
- The connected components that are solely in the bottom row are lined up sequentially, starting from the right hand side to the left of the free vertices, such that the vertices in each connected component are in consecutive order.

- The connected components that are solely in the top row are lined up sequentially, starting from the far left hand side, such that the vertices in each connected component are in consecutive order.
- The connected components between different rows are such that no two subsets cross.

**Example 9** The  $(5 + 6)\setminus 3$ -diagram



is algorithmically planar. However, the  $(5 + 6)\setminus 3$ -diagram



is not algorithmically planar because the free vertex labelled 1 is not at the far right hand side of the top row.

**Remark 34** It is clear that an algorithmically planar set partition diagram is **planar**, that is, none of the connected components in the diagram cross.

## 5.2 Multiplication Algorithm

In Algorithm 1, we outline a procedure called **MatrixMult** that performs the matrix multiplication of  $v$  by a spanning set element in  $\text{Hom}_{G(n)}((\mathbb{R}^n)^{\otimes k}, (\mathbb{R}^n)^{\otimes l})$  using the guiding principles that were given in the previous section. We assume that we have the set partition diagram that is associated with the spanning set element. Note that in the description of the algorithm, we have used  $d_\pi$  to represent a generic  $(k, l)$ -partition diagram; however, the type of set partition diagrams that we can use as input depends entirely upon the group  $G(n)$ . For example, if  $G(n) = O(n)$ , then only  $(k, l)$ -Brauer diagrams are valid as inputs to the procedure.

We now describe each of the subprocedures that appear in Algorithm 1 in more detail.

**Factor** takes as input a  $(k, l)$ -partition diagram that is appropriate for the group  $G(n)$ . The procedure uses the string-like property of these diagrams to output three diagrams whose composition is equivalent to the original input diagram. The first is a  $(k, k)$ -partition diagram that corresponds to a permutation  $\sigma_k \in S_k$ . Specifically, if  $i$  is a vertex in the top row, then the vertex in the bottom row that is connected to it is  $k + \sigma_k(i)$ . The second is a  $(k, l)$ -partition diagram that is algorithmically planar. The third is an  $(l, l)$ -partition diagram which can be interpreted as a permutation  $\sigma_l \in S_l$  in the same way as the first diagram, replacing  $k$  with  $l$ .

**Permute** takes as input a vector  $w \in (\mathbb{R}^n)^{\otimes m}$ , for some  $n, m$ , that is expressed in the standard basis of  $\mathbb{R}^n$ , and a permutation  $\sigma$  in  $S_m$ , and outputs another vector in  $(\mathbb{R}^n)^{\otimes m}$  where only the indices of the basis vectors – and not the indices of the coefficients of  $w$  – have

**Algorithm 1: MatrixMult**( $G(n), d_\pi, v$ )**Inputs:**

- $G(n)$  is a group.
- $d_\pi$  is an appropriate  $(k, l)$ -partition diagram for  $G(n)$ .
- $v \in (\mathbb{R}^n)^{\otimes k}$ .

**Perform the following steps:**

1.  $\sigma_k, d_\pi, \sigma_l \leftarrow \mathbf{Factor}(G(n), d_\pi)$
2.  $v \leftarrow \mathbf{Permute}(v, \sigma_k)$
3.  $w \leftarrow \mathbf{PlanarMult}(G(n), d_\pi, v)$
4.  $w \leftarrow \mathbf{Permute}(w, \sigma_l)$

**Output:**  $w \in (\mathbb{R}^n)^{\otimes l}$ .

been permuted according to  $\sigma$ . Said differently, **Permute** performs the following operation, which is extended linearly:

$$\sigma \cdot w_I e_I := w_I (e_{i_{\sigma(1)}} \otimes e_{i_{\sigma(2)}} \otimes \cdots \otimes e_{i_{\sigma(m)}}) \quad (90)$$

Note that in Algorithm 1,  $m$  will be equal to either  $k$  or  $l$ .

**PlanarMult** takes as input an algorithmically planar set partition diagram of the form returned by **Factor** together with a vector, and performs a fast matrix multiplication on this vector. Since the set partition diagram is algorithmically planar, we first use the monoidal property of the category in which it is a morphism to decompose it as a tensor product of smaller set partition diagrams. Next, we apply the monoidal functor that is appropriate for  $G(n)$  to express this tensor product of diagrams as a Kronecker product of smaller matrices. Finally, we perform matrix multiplication by applying these smaller matrices to the input vector from “right-to-left, diagram-by-diagram” – to be described in more detail for each group below – returning another vector as output.

**Remark 35** *In effect, the **Factor** procedure takes as input a  $(k, l)$ -partition diagram that is appropriate for the group  $G(n)$  and swaps as many pairs of vertices as necessary in each row in order to obtain an algorithmically planar  $(k, l)$ -partition diagram. The composition of the swaps in each row is represented by a permutation diagram.*

**Remark 36** *We note that the implementation of the **Factor** and **PlanarMult** procedures vary according to the group  $G(n)$  and the type of set partition diagrams that correspond to  $G(n)$ , although they share many commonalities. We describe the implementation of these procedures for each of the groups below.*



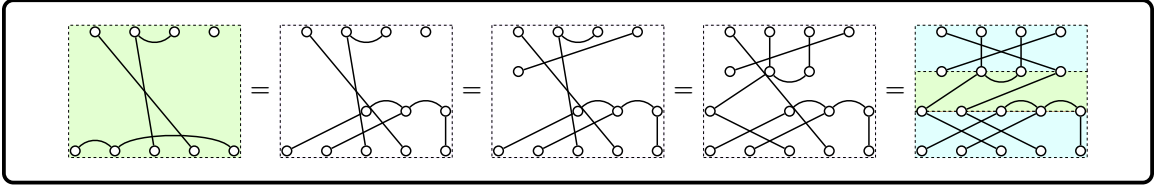


Figure 1: We use the string-like property of  $(k, l)$ -partition diagrams to **Factor** them as a composition of a permutation in  $S_k$ , an algorithmically planar  $(k, l)$ -partition diagram, and a permutation in  $S_l$ . Here,  $k = 5$  and  $l = 4$ .

**Remark 37** For each group  $G(n)$ , we also analyse the time complexity of the implementation of **MatrixMult** and compare it with the time complexity of the naive implementation of matrix multiplication. Note that in our analysis, we are viewing memory operations, such as permuting basis vectors and making copies of coefficients, as having no cost. Hence, we view the procedures **Factor** and **Permute** as having no cost. As a result, it is enough to consider the computational cost of **PlanarMult** only.

### 5.2.1 SYMMETRIC GROUP $S_n$

The implementation of Algorithm 1 that we give here for the symmetric group effectively recovers the algorithm that was presented in Godfrey et al. (2023, Appendix C); however, we take an entirely different approach that uses monoidal categories instead. The major difference in implementation between the two versions relates to how, in our terminology, the connected components between vertices in different rows of  $d_\pi$  are pulled into the middle diagram in **Factor**. We choose to make sure that the connected components do not cross, making the resulting diagram algorithmically planar, whereas in Godfrey et al. (2023) they choose to connect the vertices in different rows such that the left-most vertices in the top row of the new diagram connect to the right-most vertices in the bottom row, that is, they make the connected components cross in “opposites”. While this does not make any significant difference in terms of performing the matrix multiplication for the symmetric group – indeed, there is only a difference in how the tensor indices are ordered – our decision to make the middle diagram in the composition algorithmically planar leads to significant performance improvements when we extend our approach to the other groups below, since for these groups, we will show that these operations reduce to the identity transformation.

**Implementation** We provide specific implementations of **Factor** and **PlanarMult** for the symmetric group  $S_n$ .

**Factor:** The input is a  $(k, l)$ -partition diagram  $d_\pi$ . We drag and bend the strings representing the connected components of  $d_\pi$  to obtain three diagrams whose composition is equivalent to  $d_\pi$ : a  $(k, k)$ -partition diagram that represents a permutation  $\sigma_k$  in the symmetric group  $S_k$ ; an algorithmically planar  $(k, l)$ -partition diagram; and a  $(l, l)$ -partition diagram that represents a permutation  $\sigma_l$  in the symmetric group  $S_l$ .

To obtain the algorithmically planar  $(k, l)$ -partition diagram, we drag and bend the strings in any way such that

- the connected components that are solely in the bottom row of  $d_\pi$  are pulled up to be next to each other in the far right hand side of the bottom row of the algorithmically planar  $(k, l)$ -partition diagram, such that the connected components are ordered by their size, in decreasing order from right to left,
- the connected components that are solely in the top row of  $d_\pi$  are pulled down to be next to each other in the far left hand side of the top row of the algorithmically planar  $(k, l)$ -partition diagram, and
- the connected components between vertices in different rows of  $d_\pi$  are bent to be in between the other vertices of the algorithmically planar  $(k, l)$ -partition diagram such that no two subsets of connected components cross.

We give an example of this procedure in Figure 1.

**PlanarMult:** We take as input the algorithmically planar  $(k, l)$ -partition diagram  $d_\pi$  having at most  $n$  blocks that is the output of **Factor**, and a vector  $v \in (\mathbb{R}^n)^{\otimes k}$  that is the output of **Permute**, as per Algorithm 1.

Let  $t$  be the number of blocks that are solely in the top row of  $d_\pi$ , let  $d$  be the number of blocks that connect vertices in different rows of  $d_\pi$ , and let  $b$  be the number of blocks that are solely in the bottom row of  $d_\pi$ .

Given how **Factor** constructs the algorithmically planar  $(k, l)$ -partition diagram  $d_\pi$ , the set partition  $\pi$  corresponding to  $d_\pi$  will be of the form

$$\left( \bigcup_{i=1}^t T_i \right) \cup \left( \bigcup_{i=1}^d D_i \right) \cup \left( \bigcup_{i=1}^b B_i \right) \quad (91)$$

such that

$$|B_1| \leq |B_2| \leq \dots \leq |B_b| \quad (92)$$

where we have used  $T_i$  to refer to a top row block,  $D_i$  to refer to a different row block, and  $B_i$  to refer to a bottom row block. If we let

$$D_i := D_i^U \cup D_i^L \quad (93)$$

where  $D_i^U$  is the subset of  $D_i$  whose vertices are in the top row of  $d_\pi$ , and  $D_i^L$  is the subset of  $D_i$  whose vertices are in the bottom row of  $d_\pi$ , then we have that the vertices in each subset are given by

- $T_i = \left\{ \sum_{j=1}^{i-1} |T_j| + 1, \dots, \sum_{j=1}^i |T_j| \right\}$  for all  $i = 1 \rightarrow t$
- $D_i^U = \left\{ \sum_{j=1}^t |T_j| + \sum_{j=1}^{i-1} |D_j^U| + 1, \dots, \sum_{j=1}^t |T_j| + \sum_{j=1}^i |D_j^U| \right\}$  for all  $i = 1 \rightarrow d$ ,
- $D_i^L = \left\{ l + \sum_{j=1}^{i-1} |D_j^L| + 1, \dots, l + \sum_{j=1}^i |D_j^L| \right\}$  for all  $i = 1 \rightarrow d$ , and
- $B_i = \left\{ l + \sum_{j=1}^d |D_j^L| + \sum_{j=1}^{i-1} |B_j| + 1, \dots, l + \sum_{j=1}^d |D_j^L| + \sum_{j=1}^i |B_j| \right\}$  for all  $i = 1 \rightarrow b$ .

Note, in particular, that

$$l = \sum_{j=1}^t |T_j| + \sum_{j=1}^d |D_j^U| \quad (94)$$

and

$$k = \sum_{j=1}^d |D_j^L| + \sum_{j=1}^b |B_j| \quad (95)$$

Next, we take  $d_\pi$  and express it as a tensor product of three types of set partition diagrams. The right-most type is itself a tensor product of diagrams corresponding to the  $B_i$ ; the middle type is a single diagram corresponding to  $\bigcup_{i=1}^d D_i$ ; and the left-most type is itself a tensor product of diagrams corresponding to the  $T_i$ .

We apply the monoidal functor  $\Theta$  to this tensor product decomposition of diagrams, which returns a Kronecker product of matrices. We perform the matrix multiplication by applying the matrices “right-to-left, diagram-by-diagram”, as follows.

**Step 1: Apply each matrix corresponding to a bottom row block diagram, one-by-one, starting from the one that corresponds to  $B_b$  and ending with the one that corresponds to  $B_1$ .**

Suppose that we are performing the part of the matrix multiplication that corresponds to  $B_i$ , for some  $i = 1 \rightarrow b$ . The input will be a vector  $w \in (\mathbb{R}^n)^{\otimes k - \sum_{j=i+1}^b |B_j|}$ .

We can express  $w$  in the standard basis of  $\mathbb{R}^n$  as

$$w = \sum_{L \in [n]^{k - \sum_{j=i+1}^b |B_j|}} w_L e_L \quad (96)$$

This will be mapped to the vector  $r \in (\mathbb{R}^n)^{\otimes k - \sum_{j=i}^b |B_j|}$ , where  $r$  is of the form

$$r = \sum_{M \in [n]^{k - \sum_{j=i}^b |B_j|}} r_M e_M \quad (97)$$

and

$$r_M = \sum_{j \in [n]} w_{M, j, \dots, j} \quad (98)$$

where the number of indices  $j$  in (98) is  $|B_i|$ .

At the end of this process, we obtain a vector in  $(\mathbb{R}^n)^{\otimes k - \sum_{j=1}^b |B_j|}$ .

Note that the matrices corresponding to bottom row connected components are merely performing indexing and summation operations, that is, ultimately, tensor contractions.

**Step 2: Now apply the matrix corresponding to the middle diagram, that is, to the set  $\bigcup_{i=1}^d D_i$ .**

The input will be a vector  $w \in (\mathbb{R}^n)^{\otimes k - \sum_{j=1}^b |B_j|}$ . Using (95), we can express  $w$  in the standard basis of  $\mathbb{R}^n$  as

$$w = \sum_{j_1, \dots, j_d \in [n]} w_{j_1, \dots, j_1, j_2, \dots, j_2, \dots, j_d, \dots, j_d} \bigotimes_{k=1}^d \left( \bigotimes_{p=1}^{|D_k^L|} e_{j_k} \right) \quad (99)$$

where each index  $j_k$  in the coefficient is repeated  $|D_k^L|$  times.

This will be mapped to the vector  $r \in (\mathbb{R}^n)^{\otimes \sum_{j=i}^d |D_j^U|}$ , where  $r$  is of the form

$$r = \sum_{j_1, \dots, j_d \in [n]} r_{j_1, \dots, j_1, j_2, \dots, j_2, \dots, j_d, \dots, j_d} \bigotimes_{k=1}^d \left( \bigotimes_{p=1}^{|D_k^U|} e_{j_k} \right) \quad (100)$$

where each index  $j_k$  in the coefficient is repeated  $|D_k^U|$  times, and

$$r_{j_1, \dots, j_1, j_2, \dots, j_2, \dots, j_d, \dots, j_d} = w_{j_1, \dots, j_1, j_2, \dots, j_2, \dots, j_d, \dots, j_d} \quad (101)$$

These operations are called transfer operations, which is a term that first appeared in Pan and Kondor (2022).

**Step 3: Finally, apply each matrix corresponding to a top row block diagram, one-by-one, starting from the one that corresponds to  $T_t$  and ending with the one that corresponds to  $T_1$ .**

Suppose that we are performing the part of the matrix multiplication that corresponds to  $T_i$ , for some  $i = 1 \rightarrow t$ .

Then we begin with a vector  $x \in (\mathbb{R}^n)^{\otimes l - \sum_{j=1}^i |T_j|}$  that is of the form

$$x = \sum_{l_{i+1}, \dots, l_t \in [n]} \sum_{j_1, \dots, j_d \in [n]} x_{j_1, j_2, \dots, j_d} \bigotimes_{q=i+1}^t \left( \bigotimes_{m=1}^{|T_q|} e_{l_q} \right) \bigotimes_{k=1}^d \left( \bigotimes_{p=1}^{|D_k^U|} e_{j_k} \right) \quad (102)$$

where  $x_{j_1, j_2, \dots, j_d}$  is the coefficient  $r_{j_1, \dots, j_1, j_2, \dots, j_2, \dots, j_d, \dots, j_d}$  appearing in (101).

This will be mapped to the vector  $y \in (\mathbb{R}^n)^{\otimes l - \sum_{j=1}^{i-1} |T_j|}$ , where  $y$  is of the form

$$y = \sum_{l_i, l_{i+1}, \dots, l_t \in [n]} \sum_{j_1, \dots, j_d \in [n]} x_{j_1, j_2, \dots, j_d} \bigotimes_{q=i}^t \left( \bigotimes_{m=1}^{|T_q|} e_{l_q} \right) \bigotimes_{k=1}^d \left( \bigotimes_{p=1}^{|D_k^U|} e_{j_k} \right) \quad (103)$$

At the end of this process, we obtain a vector in  $(\mathbb{R}^n)^{\otimes l}$ , by (94), which is of the form

$$\sum_{l_1, \dots, l_t \in [n]} \sum_{j_1, \dots, j_d \in [n]} x_{j_1, j_2, \dots, j_d} \bigotimes_{q=1}^t \left( \bigotimes_{m=1}^{|T_q|} e_{l_q} \right) \bigotimes_{k=1}^d \left( \bigotimes_{p=1}^{|D_k^U|} e_{j_k} \right) \quad (104)$$

This is the vector that is returned by **PlanarMult** for the symmetric group  $S_n$ .

To summarise, the implementation of **PlanarMult** for the symmetric group  $S_n$  takes as input the algorithmically planar  $(k, l)$ -partition diagram that comes from **Factor** and expresses it as a tensor product of three types of set partition diagrams. The right-most type is itself a tensor product of set partition diagrams having only vertices in the bottom row, where each diagram represents a single block. These diagrams correspond to tensor contraction operations under the functor  $\Theta$ . The middle type is a set partition diagram that consists of all of the connected components in the algorithmically planar  $(k, l)$ -partition diagram between vertices in different rows. These diagrams correspond to transfer operations under the functor  $\Theta$ . The left-most type is itself a tensor product of set partition diagrams

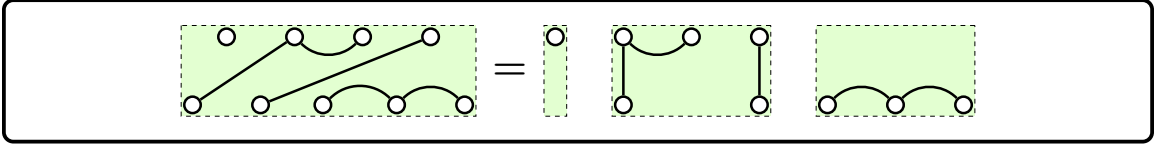


Figure 2: The decomposition of the algorithmically planar  $(5, 4)$ -partition diagram that appears in Figure 1 into a tensor product of smaller partition diagrams. These diagrams correspond, from right-to-left, to tensor contraction, transfer, and copying operations under the functor  $\Theta$ . This tensor product decomposition is used in **PlanarMult** for the symmetric group  $S_n$ .

having only vertices in the top row, where each diagram represents a single block. These diagrams correspond to indexing operations that perform copies under the functor  $\Theta$ .

In Figure 2, we present the tensor product decomposition of the algorithmically planar  $(5, 4)$ -partition diagram that is shown in Figure 1.

To show diagrammatically how the matrix multiplication is performed, we see that the tensor product of the three types of set partition diagrams corresponds to a Kronecker product of smaller matrices under the functor  $\Theta$ , defined in Theorem 27, by the monoidal property of  $\Theta$ . We would like to apply each smaller matrix to the input vector from right-to-left, diagram-by-diagram. To do this, we first deform the entire tensor product decomposition of set partition diagrams by pulling each individual diagram up one level higher than the previous one, going from right-to-left, and then apply the functor  $\Theta$  at each level. The newly inserted strings correspond to an identity matrix, hence only the matrices corresponding to the original tensor product decomposition act on the input vector at each stage.

Figure 3 gives an example of how the computation takes place at each stage for the tensor product decomposition given in Figure 2, using its equivalent diagram form.

**Example 10** Suppose that we wish to perform the multiplication of  $D_\pi$  by  $v \in (\mathbb{R}^n)^{\otimes 5}$ , where  $D_\pi$  corresponds to the  $(5, 4)$ -partition diagram  $d_\pi$  given in Figure 1 under  $\Theta$ , and  $v$  is given by

$$\sum_{L \in [n]^5} v_L e_L \quad (105)$$

We know that  $D_\pi$  is a matrix in  $\text{Hom}_{S_n}((\mathbb{R}^n)^{\otimes 5}, (\mathbb{R}^n)^{\otimes 4})$ .

First, we apply the procedure **Factor**, which returns the three diagrams given in Figure 1. The first diagram corresponds to the permutation  $(13)(24)$  in  $S_5$ ; hence, the result of **Permute** $(v, (13)(24))$  is the vector

$$\sum_{L \in [n]^5} v_{l_1, l_2, l_3, l_4, l_5} (e_{l_3} \otimes e_{l_4} \otimes e_{l_1} \otimes e_{l_2} \otimes e_{l_5}) \quad (106)$$

Next we apply **PlanarMult** with the decomposition given in Figure 2.

*Step 1: Apply the matrices that correspond to the bottom row blocks.*

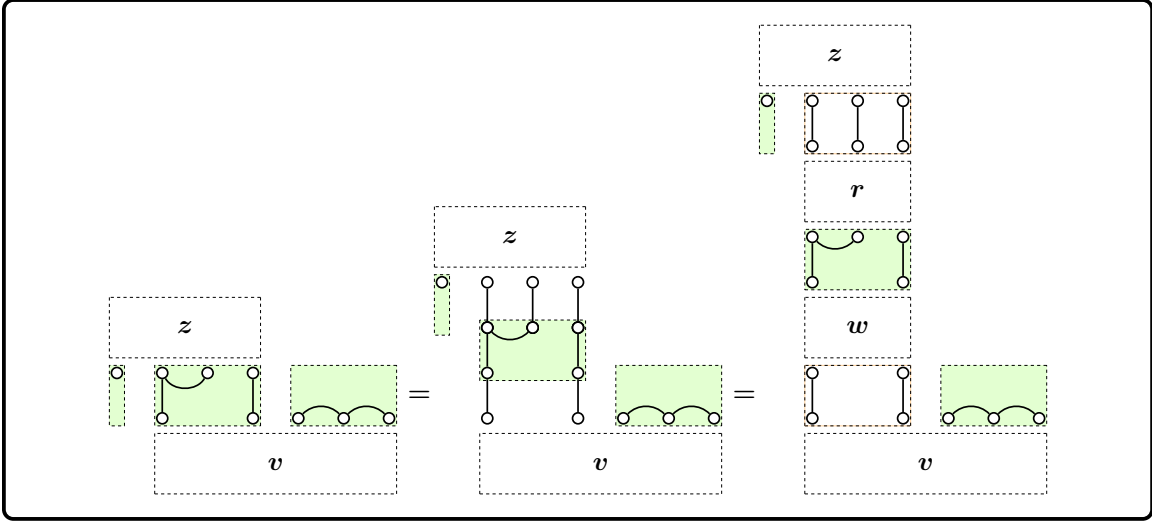


Figure 3: We show how matrix multiplication is implemented in **PlanarMult** for  $S_n$  using the tensor product decomposition of the algorithmically planar  $(5, 4)$ -partition diagram given in Figure 2 as an example. We perform the matrix multiplication as follows: first, we deform the entire tensor product decomposition diagram by pulling each individual diagram up one level higher than the previous one, going from right-to-left, and then we apply the functor  $\Theta$  at each level. Finally, we perform matrix multiplication at each level to obtain the final output vector.

We obtain the vector

$$w = \sum_{l_3, l_4 \in [n]} w_{l_3, l_4} (e_{l_3} \otimes e_{l_4}) \quad (107)$$

where

$$w_{l_3, l_4} = \sum_{j \in [n]} v_{j, j, l_3, l_4, j} \quad (108)$$

Step 2: Apply the matrices that correspond to the middle diagram.

We obtain the vector

$$r = \sum_{l_3 \in [n]} \sum_{l_4 \in [n]} r_{l_3, l_3, l_4} (e_{l_3} \otimes e_{l_3} \otimes e_{l_4}) \quad (109)$$

where

$$r_{l_3, l_3, l_4} = w_{l_3, l_4} \quad (110)$$

Step 3: Apply the matrices that correspond to the top row blocks.

We obtain the vector

$$z = \sum_{m \in [n]} \sum_{l_3 \in [n]} \sum_{l_4 \in [n]} r_{l_3, l_3, l_4} (e_m \otimes e_{l_3} \otimes e_{l_3} \otimes e_{l_4}) \quad (111)$$

Substituting in, we get that

$$z = \sum_{m \in [n]} \sum_{l_3 \in [n]} \sum_{l_4 \in [n]} w_{l_3, l_4} (e_m \otimes e_{l_3} \otimes e_{l_3} \otimes e_{l_4}) \quad (112)$$

and hence

$$z = \sum_{m \in [n]} \sum_{l_3 \in [n]} \sum_{l_4 \in [n]} \sum_{j \in [n]} v_{j, j, l_3, l_4, j} (e_m \otimes e_{l_3} \otimes e_{l_3} \otimes e_{l_4}) \quad (113)$$

Finally, as the third diagram returned from **Factor** corresponds to the permutation (14) in  $S_4$ , we perform **Permute**( $z$ , (14)), which returns the vector

$$z = \sum_{m \in [n]} \sum_{l_3 \in [n]} \sum_{l_4 \in [n]} \sum_{j \in [n]} v_{j, j, l_3, l_4, j} (e_{l_4} \otimes e_{l_3} \otimes e_{l_3} \otimes e_m) \quad (114)$$

This is the vector that is returned by **MatrixMult**.

**Time Complexity** We look at each step of the implementation that was given above.

**Step 1:** For the part of the matrix multiplication that corresponds to  $B_i$ , for some  $i = 1 \rightarrow b$ , we map a vector in  $(\mathbb{R}^n)^{\otimes k - \sum_{j=i+1}^b |B_j|}$  to a vector in  $(\mathbb{R}^n)^{\otimes k - \sum_{j=i}^b |B_j|}$ .

Since the matrix corresponds to a bottom row block, for each tuple  $M$  of indices in the output coefficient  $r_M$ , as in (98), there are only  $n$  terms to multiply (an improvement over  $n^{|B_i|}$ ), and consequently only  $n - 1$  additions.

Hence, in total, there are

$$\sum_{i=1}^b n^{k - \sum_{j=b+1-i}^b |B_j|} \cdot n \quad (115)$$

multiplications and

$$\sum_{i=1}^b n^{k - \sum_{j=b+1-i}^b |B_j|} \cdot (n - 1) \quad (116)$$

additions. Note that, in calculating the overall time complexity for this step, the highest order term is given by the size of  $B_b$ . Hence, the worst case occurs when  $|B_b| = 1$ , giving an overall time complexity of  $O(n^k)$ . However, assuming that Step 1 must take place, the best case occurs when  $|B_b| = k$ , that is, there is only one bottom row block of size  $k$ , giving an overall time complexity of  $O(n)$ .

**Step 2:** As these are transfer operations, there is no cost since we are simply copying elements from an array.

**Step 3:** Here we are copying arrays, hence there is no cost.

Consequently, in the worst case, we have reduced the overall time complexity from  $O(n^{l+k})$  to  $O(n^k)$ . If Step 1 must occur, then in the best case, we have reduced the overall time complexity from  $O(n^{l+k})$  to  $O(n)$ . However, the true best case occurs when Step 1 does not take place at all, that is, when the number of bottom row blocks  $b$  is zero, because, in this case, the computation is effectively free!

This analysis also shows why, in Definition 31 of an algorithmically planar  $(k, l)$ -partition diagram, we have chosen to order the connected components that are solely in the bottom row by their size, in decreasing order from right to left. We want to obtain the best

overall time complexity for the multiplication algorithm, which, for the symmetric group, is determined by the number of additions and multiplications that occur in Step 1. It is clear from (115) and (116) that the time complexity is best when the blocks are ordered in decreasing size order from right to left.

### 5.2.2 ORTHOGONAL GROUP $O(n)$

The implementation of Algorithm 1 for the orthogonal group  $O(n)$  is similar to the implementation for the symmetric group  $S_n$  as a result of the similarity between the monoidal functors that are associated with each group. In fact, the implementation for the orthogonal group will be less involved because the only valid set partition diagrams that can be input into the **MatrixMult** procedure for this group are Brauer diagrams.

**Implementation** We provide specific implementations of **Factor** and **PlanarMult** for the orthogonal group  $O(n)$ .

**Factor:** The input is a  $(k, l)$ -Brauer diagram  $d_\beta$ . We drag and bend the strings representing the connected components of  $d_\beta$  to obtain a factoring of  $d_\beta$  into three diagrams whose composition is equivalent to  $d_\beta$ : a  $(k, k)$ -Brauer diagram that represents a permutation  $\sigma_k$  in the symmetric group  $S_k$ ; another  $(k, l)$ -Brauer diagram that is algorithmically planar; and a  $(l, l)$ -Brauer diagram that represents a permutation  $\sigma_l$  in the symmetric group  $S_l$ .

To obtain the algorithmically planar  $(k, l)$ -Brauer diagram, we drag and bend the strings in any way such that

- the pairs that are solely in the bottom row of  $d_\beta$  are pulled up to be next to each other in the far right hand side of the bottom row of the algorithmically planar  $(k, l)$ -Brauer diagram,
- the pairs that are solely in the top row of  $d_\beta$  are pulled down to be next to each other in the far left hand side of the top row of the algorithmically planar  $(k, l)$ -Brauer diagram, and
- the pairs between vertices in different rows of  $d_\beta$  are bent to be in between the other vertices of the algorithmically planar  $(k, l)$ -Brauer diagram such that no two pairings in the algorithmically planar diagram intersect each other.

We give an example of this procedure in Figure 4.

**PlanarMult:** We take as input the planar  $(k, l)$ -Brauer diagram  $d_\beta$  that is the output of **Factor**, and a vector  $v \in (\mathbb{R}^n)^{\otimes k}$  that is the output of **Permute**, as per Algorithm 1.

Let  $t$  be the number of pairs that are solely in the top row of  $d_\beta$ , let  $d$  be the number of pairs that are in different rows of  $d_\beta$ , and let  $b$  be the number of pairs that are solely in the bottom row of  $d_\beta$ .

Then it is clear that

$$2t + d = l \quad \text{and} \quad 2b + d = k \tag{117}$$

and so

$$2t + 2d + 2b = l + k \tag{118}$$



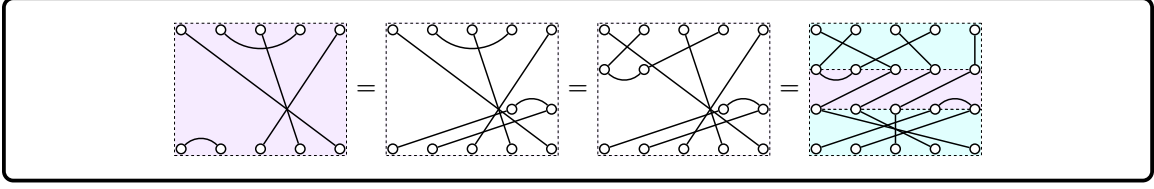


Figure 4: We use the string-like aspect of  $(k, l)$ -Brauer diagrams to **Factor** them as a composition of a permutation in  $S_k$ , an algorithmically planar  $(k, l)$ -Brauer diagram, and a permutation in  $S_l$ . Here  $k = l = 5$ .

Given how **Factor** constructs the planar  $(k, l)$ -Brauer diagram  $d_\beta$ , the Brauer partition  $\beta$  corresponding to  $d_\beta$  will be of the form

$$\left( \bigcup_{i=1}^t T_i \right) \cup \left( \bigcup_{i=1}^d D_i \right) \cup \left( \bigcup_{i=1}^b B_i \right) \quad (119)$$

where we have used  $T_i$  to refer to a top row pair,  $D_i$  to refer to a different row pair, and  $B_i$  to refer to a bottom row pair. In particular, we have that

- $T_i = \{2i - 1, 2i\}$  for all  $i = 1 \rightarrow t$
- $D_i = \{l + i - d, l + i\}$  for all  $i = 1 \rightarrow d$ , and
- $B_i = \{l + k - 2b + 2i - 1, l + k - 2b + 2i\}$  for all  $i = 1 \rightarrow b$ .

Next, we take  $d_\beta$  and express it as a tensor product of three types of Brauer diagrams. The right-most type is itself a tensor product of diagrams corresponding to the  $B_i$ ; the middle type is a single diagram corresponding to  $\bigcup_{i=1}^d D_i$ ; and the left-most type is itself a tensor product of diagrams corresponding to the  $T_i$ .

We apply the monoidal functor  $\Phi$  to this tensor product decomposition of diagrams, which returns a Kronecker product of matrices. We perform the matrix multiplication by applying the matrices “right-to-left, diagram-by-diagram”, as follows.

**Step 1: Apply each matrix corresponding to a bottom row pair diagram, one-by-one, starting from the one that corresponds to  $B_b$  and ending with the one that corresponds to  $B_1$ .**

Suppose that we are performing the part of the matrix multiplication that corresponds to  $B_i$ , for some  $i = 1 \rightarrow b$ . The input will be a vector  $w \in (\mathbb{R}^n)^{\otimes k-2(b-i)}$ .

We can express  $w$  in the standard basis of  $\mathbb{R}^n$  as

$$w = \sum_{L \in [n]^{k-2(b-i)}} w_L e_L \quad (120)$$

This will be mapped to the vector  $r \in (\mathbb{R}^n)^{\otimes k-2(b-i)-2}$ , where  $r$  is of the form

$$r = \sum_{M \in [n]^{k-2(b-i)-2}} r_M e_M \quad (121)$$

and

$$r_M = \sum_{j \in [n]} w_{M,j,j} \quad (122)$$

At the end of this process, we obtain a vector in  $(\mathbb{R}^n)^{\otimes k-2b}$ .

As before, the matrices corresponding to bottom row pairs are merely performing tensor contractions.

**Step 2: Now apply the matrix corresponding to the middle diagram, that is, to the set  $\bigcup_{i=1}^d D_i$ .**

The input will be a vector  $w \in (\mathbb{R}^n)^{\otimes k-2b}$ .

Expressing  $w$  in the standard basis of  $\mathbb{R}^n$  as

$$w = \sum_{L \in [n]^{k-2b}} w_L e_L \quad (123)$$

the multiplication of the matrix merely returns  $w$  itself!

Hence the transfer operations for the orthogonal group are simply the identity map.

**Step 3: Finally, apply each matrix corresponding to a top row pair diagram, one-by-one, starting from the one that corresponds to  $T_t$  and ending with the one that corresponds to  $T_1$ .**

Suppose that we are performing the part of the matrix multiplication that corresponds to  $T_i$ , for some  $i = 1 \rightarrow t$ .

Then we begin with a vector  $w \in (\mathbb{R}^n)^{\otimes k-2b+2(t-i)}$  that is of the form

$$w = \sum_{J \in [n]^{t-i}} \sum_{L \in [n]^{k-2b}} v_L (e_{j_1} \otimes e_{j_1} \otimes \cdots \otimes e_{j_{t-i}} \otimes e_{j_{t-i}} \otimes e_L) \quad (124)$$

where  $v_L$  is the coefficient of  $e_L$  appearing in the vector at the end of Step 2.

This will be mapped to the vector  $r \in (\mathbb{R}^n)^{\otimes k-2b+2(t-i)+2}$ , where  $r$  is of the form

$$r = \sum_{m \in [n]} \sum_{J \in [n]^{t-i}} \sum_{L \in [n]^{k-2b+2(t-i)}} v_L (e_m \otimes e_m \otimes e_{j_1} \otimes e_{j_1} \otimes \cdots \otimes e_{j_{t-i}} \otimes e_{j_{t-i}} \otimes e_L) \quad (125)$$

At the end of this process, we obtain a vector in  $(\mathbb{R}^n)^{\otimes l}$ , since  $k - 2b + 2t = l$ , which is of the form

$$\sum_{J \in [n]^t} \sum_{L \in [n]^{k-2b}} v_L (e_{j_1} \otimes e_{j_1} \otimes \cdots \otimes e_{j_t} \otimes e_{j_t} \otimes e_L) \quad (126)$$

This is the vector that is returned by **PlanarMult** for the orthogonal group  $O(n)$ .

To summarise, the implementation of **PlanarMult** for the orthogonal group  $O(n)$  takes as input the algorithmically planar  $(k, l)$ -Brauer diagram that comes from **Factor** and expresses it as a tensor product of three types of Brauer diagrams. The right-most type is itself a tensor product of Brauer diagrams, where each diagram has only two connected vertices in the bottom row. These diagrams correspond to tensor contraction operations under the functor  $\Phi$  given in Theorem 28. The middle type is a Brauer diagram that consists of all of the pairs in the planar  $(k, l)$ -Brauer diagram between vertices in different rows. This diagram corresponds to the identity under the functor  $\Phi$ . The left-most type

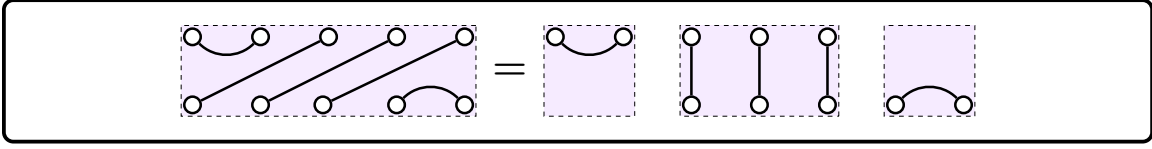


Figure 5: The tensor product decomposition of the planar  $(5, 5)$ -Brauer diagram that appears in Figure 4.

is a tensor product of Brauer diagrams having only two connected vertices in the top row. These diagrams correspond to indexing operations that perform copies under the functor  $\Phi$ .

In Figure 5, we present the tensor product decomposition of the algorithmically planar  $(5, 5)$ -Brauer diagram that is shown in Figure 4.

The diagrammatic representation of the matrix multiplication step is very similar to the one for the symmetric group, in that to obtain the matrices we perform the same deformation of the tensor product decomposition of diagrams before applying the functor  $\Phi$  at each level. We give an example in Figure 6 of how the computation takes place at each stage for the tensor product decomposition given in Figure 5, using its equivalent diagram form.

**Example 11** Suppose that we wish to perform the multiplication of  $E_\beta$  by  $v \in (\mathbb{R}^n)^{\otimes 5}$ , where  $E_\beta$  corresponds to the  $(5, 5)$ -Brauer diagram  $d_\beta$  given in Figure 4 under  $\Phi$ , and  $v$  is given by

$$\sum_{L \in [n]^5} v_L e_L \quad (127)$$

We know that  $E_\beta$  is a matrix in  $\text{Hom}_{O(n)}((\mathbb{R}^n)^{\otimes 5}, (\mathbb{R}^n)^{\otimes 5})$ .

First, we apply the procedure **Factor**, which returns the three diagrams given in Figure 4. The first diagram corresponds to the permutation  $(1524)$  in  $S_5$ , hence, the result of **Permute** $(v, (1524))$  is the vector

$$\sum_{L \in [n]^5} v_{l_1, l_2, l_3, l_4, l_5} (e_{l_5} \otimes e_{l_4} \otimes e_{l_3} \otimes e_{l_1} \otimes e_{l_2}) \quad (128)$$

Now we apply **PlanarMult** with the decomposition given in Figure 5.

*Step 1:* Apply the matrices that correspond to the bottom row pairs.

We obtain the vector

$$w = \sum_{l_5, l_4, l_3 \in [n]} w_{l_5, l_4, l_3} (e_{l_5} \otimes e_{l_4} \otimes e_{l_3}) \quad (129)$$

where

$$w_{l_5, l_4, l_3} = \sum_{j \in [n]} v_{j, j, l_3, l_4, l_5} \quad (130)$$

*Step 2:* Apply the matrices that correspond to the middle diagram.

As the transfer operations are the identity mapping, we get  $w$ .

*Step 3:* Apply the matrices that correspond to the top row.

We obtain the vector

$$z = \sum_{m \in [n]} \sum_{l_5, l_4, l_3 \in [n]} w_{l_5, l_4, l_3} (e_m \otimes e_m \otimes e_{l_5} \otimes e_{l_4} \otimes e_{l_3}) \quad (131)$$

Substituting in, we get that

$$z = \sum_{m \in [n]} \sum_{l_5, l_4, l_3 \in [n]} \sum_{j \in [n]} v_{j, l_3, l_4, l_5} (e_m \otimes e_m \otimes e_{l_5} \otimes e_{l_4} \otimes e_{l_3}) \quad (132)$$

Finally, as the third diagram returned from **Factor** corresponds to the permutation (1342) in  $S_5$ , we perform **Permute**( $z, (1342)$ ), which returns the vector

$$\sum_{m \in [n]} \sum_{l_5, l_4, l_3 \in [n]} \sum_{j \in [n]} v_{j, l_3, l_4, l_5} (e_{l_5} \otimes e_m \otimes e_{l_4} \otimes e_m \otimes e_{l_3}) \quad (133)$$

This is the vector that is returned by **MatrixMult**.

**Time Complexity** We look at each step of the implementation that was given above.

**Step 1:** For the part of the matrix multiplication that corresponds to  $B_i$ , for some  $i = 1 \rightarrow b$ , we map a vector in  $(\mathbb{R}^n)^{\otimes k-2(b-i)}$  to a vector in  $(\mathbb{R}^n)^{\otimes k-2(b-i)-2}$ .

Since the matrix corresponds to a bottom row pair that is connected, for each tuple  $M$  of indices in the output coefficient  $r_M$ , as in (122), there are only  $n$  terms to multiply (an improvement over  $n^2$ ), and consequently only  $n - 1$  additions.

Hence, in total, there are

$$\sum_{i=1}^b n^{k-2(b-i)-2} \cdot n \quad (134)$$

multiplications and

$$\sum_{i=1}^b n^{k-2(b-i)-2} \cdot (n - 1) \quad (135)$$

additions, for an overall time complexity of  $O(n^{k-1})$ .

**Step 2:** This corresponds to the identity transformation, hence there is no cost, as we do not need to perform this operation.

**Step 3:** Here we are copying arrays, hence there is no cost.

Consequently, we have reduced the overall time complexity from  $O(n^{l+k})$  to  $O(n^{k-1})$ .

### 5.2.3 SYMPLECTIC GROUP $Sp(n)$

The implementation of Algorithm 1 for the symplectic group  $Sp(n)$  is related to the implementation for the orthogonal group  $O(n)$  because the only valid set partition diagrams that can be input into the procedure in each case are Brauer diagrams. The difference in the implementations comes from the difference in the monoidal functor that is associated with each group.

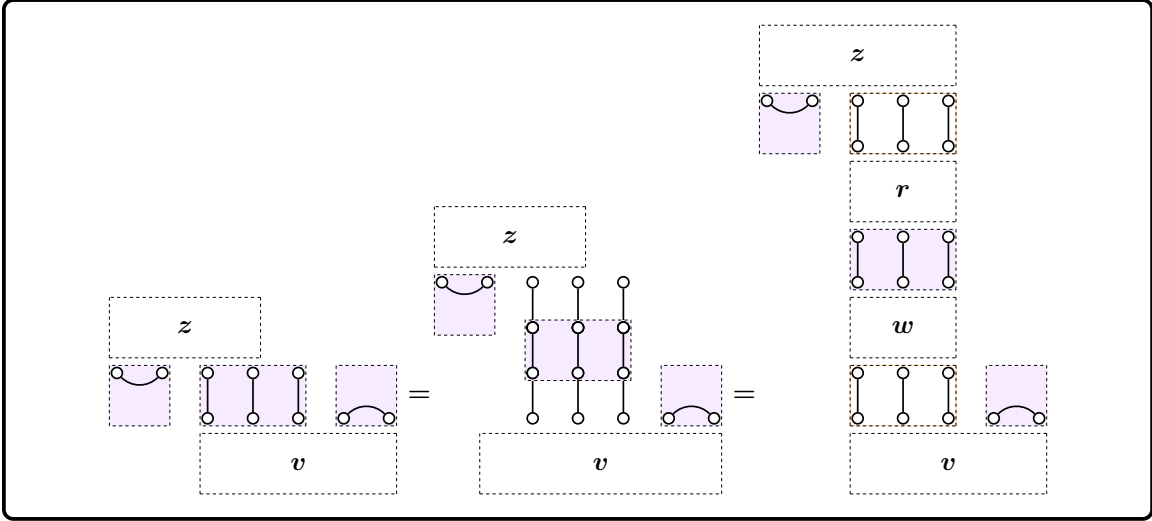


Figure 6: We show how matrix multiplication is implemented in **PlanarMult** for  $O(n)$ ,  $Sp(n)$  and  $SO(n)$  using the tensor product decomposition of the planar  $(5, 5)$ -Brauer diagram given in Figure 5 as an example. Effectively, we perform the matrix multiplication by applying the matrices “right-to-left, diagram-by-diagram”. In reality, we perform the matrix multiplication as follows: first, we deform the entire tensor product decomposition diagram by pulling each individual diagram up one level higher than the previous one, going from right-to-left, and then we apply the functor that corresponds to the group at each level. Finally, we perform matrix multiplication at each level to obtain the final output vector.

**Implementation** The implementation of the **Factor** procedure is the same as for the orthogonal group.

**PlanarMult:** Again, we take as input the planar  $(k, l)$ -Brauer diagram  $d_\beta$  that is the output of **Factor**, and a vector  $v \in (\mathbb{R}^n)^{\otimes k}$  that is the output of **Permute**, as per Algorithm 1.

The tensor product decomposition of  $d_\beta$  is the same as for the orthogonal group  $O(n)$ ; in particular, the Brauer partition  $\beta$  corresponding to  $d_\beta$  is of the form (119). The important difference here is that we apply the monoidal functor  $X$ , instead of  $\Phi$ , to this tensor product decomposition of diagrams, which returns a different Kronecker product of matrices. Again, we perform the same steps for the matrix multiplication, but this time the vectors returned at each stage are different.

**Step 1: Apply each matrix corresponding to a bottom row pair diagram, one-by-one, starting from the one that corresponds to  $B_b$  and ending with the one that corresponds to  $B_1$ .**

Suppose that we are performing the part of the matrix multiplication that corresponds to  $B_i$ , for some  $i = 1 \rightarrow b$ . The input will be a vector  $w \in (\mathbb{R}^n)^{\otimes k-2(b-i)}$ .

We can express  $w$  in the standard basis of  $\mathbb{R}^n$  as

$$w = \sum_{L \in [n]^{k-2(b-i)}} w_L e_L \quad (136)$$

This will be mapped to the vector  $r \in (\mathbb{R}^n)^{\otimes k-2(b-i)-2}$  where  $r$  is of the form

$$r = \sum_{M \in [n]^{k-2(b-i)-2}} r_M e_M \quad (137)$$

where

$$r_M = \sum_{j_{k-2(b-i)-1}, j_{k-2(b-i)} \in [n]} \epsilon_{j_{k-2(b-i)-1}, j_{k-2(b-i)}} w_{M, j_{k-2(b-i)-1}, j_{k-2(b-i)}} \quad (138)$$

Recall that  $\epsilon_{j_{k-2(b-i)-1}, j_{k-2(b-i)}}$  was defined in (24) and (25).

At the end of this process, we obtain a vector in  $(\mathbb{R}^n)^{\otimes k-2b}$ .

As before, these matrices corresponding to bottom row pairs are performing tensor contractions.

**Step 2: Now apply the matrix corresponding to the middle diagram, that is, to the set  $\bigcup_{i=1}^d D_i$ .**

This will be exactly the same as for the orthogonal group, by the definition of  $\gamma_{r_p, u_p}$  given in (23).

**Step 3: Finally, apply each matrix corresponding to a top row pair diagram, one-by-one, starting from the one that corresponds to  $T_t$  and ending with the one that corresponds to  $T_1$ .**

Suppose that we are performing the part of the matrix multiplication that corresponds to  $T_i$ , for some  $i = 1 \rightarrow t$ .

Then we begin with a vector  $w \in (\mathbb{R}^n)^{\otimes k-2b+2(t-i)}$  that is of the form

$$w = \sum_{J \in [n]^{2(t-i)}} \sum_{L \in [n]^{k-2b}} \epsilon_{J\nu L} (e_J \otimes e_L) \quad (139)$$

where

$$\epsilon_J := \epsilon_{j_1, j_2} \cdots \epsilon_{j_{2(t-i)-1}, j_{2(t-i)}} \quad (140)$$

and where  $\nu_L$  is the coefficient of  $e_L$  appearing in the vector at the end of Step 2.

This will be mapped to the vector  $r \in (\mathbb{R}^n)^{\otimes k-2b+2(t-i)+2}$ , where  $r$  is of the form

$$r = \sum_{M \in [n]^2} \sum_{J \in [n]^{2(t-i)}} \sum_{L \in [n]^{k-2b}} \epsilon_{M, J\nu L} (e_M \otimes e_J \otimes e_L) \quad (141)$$

where

$$\epsilon_{M, J} := \epsilon_{m_1, m_2} \epsilon_{j_1, j_2} \cdots \epsilon_{j_{2(t-i)-1}, j_{2(t-i)}} \quad (142)$$

At the end of this process, we obtain a vector in  $(\mathbb{R}^n)^{\otimes l}$ , since  $k - 2b + 2t = l$ , which is of the form

$$\sum_{J \in [n]^{2t}} \sum_{L \in [n]^{k-2b}} \epsilon_{J\nu L} (e_J \otimes e_L) \quad (143)$$

where  $\epsilon_J$  is redefined to be

$$\epsilon_{j_1, j_2} \cdots \epsilon_{j_{2t-1}, j_{2t}} \quad (144)$$

This is the vector that is returned by **PlanarMult** for the symplectic group  $Sp(n)$ .

**Example 12** Suppose that we wish to perform the multiplication of  $F_\beta$  by  $v \in (\mathbb{R}^n)^{\otimes 5}$ , for the same  $(5, 5)$ -Brauer diagram  $d_\beta$  given in Figure 4, and  $v$  is given by

$$\sum_{L \in [n]^5} v_L e_L \quad (145)$$

We know that  $F_\beta$  is a matrix in  $\text{Hom}_{Sp(n)}((\mathbb{R}^n)^{\otimes 5}, (\mathbb{R}^n)^{\otimes 5})$ .

The **Factor** and **Permute** steps are the same as for Example 11, hence, prior to the **PlanarMult** step, we have the vector

$$\sum_{L \in [n]^5} v_{l_1, l_2, l_3, l_4, l_5} (e_{l_5} \otimes e_{l_4} \otimes e_{l_3} \otimes e_{l_1} \otimes e_{l_2}) \quad (146)$$

We now apply **PlanarMult** with the decomposition given in Figure 5.

*Step 1:* Apply the matrices that correspond to the bottom row pairs.

We obtain the vector

$$w = \sum_{l_5, l_4, l_3 \in [n]} w_{l_5, l_4, l_3} (e_{l_5} \otimes e_{l_4} \otimes e_{l_3}) \quad (147)$$

where

$$w_{l_5, l_4, l_3} = \sum_{j_1, j_2 \in [n]} \epsilon_{j_1, j_2} v_{j_1, j_2, l_3, l_4, l_5} \quad (148)$$

*Step 2:* Apply the matrices that correspond to the middle diagram.

As the transfer operations are the identity mapping, we get  $w$ .

*Step 3:* Apply the matrices that correspond to the top row.

We obtain the vector

$$z = \sum_{m_1, m_2 \in [n]} \sum_{l_5, l_4, l_3 \in [n]} \epsilon_{m_1, m_2} w_{l_5, l_4, l_3} (e_{m_1} \otimes e_{m_2} \otimes e_{l_5} \otimes e_{l_4} \otimes e_{l_3}) \quad (149)$$

Substituting in, we get that

$$z = \sum_{m_1, m_2 \in [n]} \sum_{l_5, l_4, l_3 \in [n]} \sum_{j_1, j_2 \in [n]} \epsilon_{m_1, m_2} \epsilon_{j_1, j_2} v_{j_1, j_2, l_3, l_4, l_5} (e_{m_1} \otimes e_{m_2} \otimes e_{l_5} \otimes e_{l_4} \otimes e_{l_3}) \quad (150)$$

Finally, as the third diagram returned from **Factor** corresponds to the permutation (1342) in  $S_5$ , we perform **Permute**( $z$ , (1342)), which returns the vector

$$\sum_{m_1, m_2 \in [n]} \sum_{l_5, l_4, l_3 \in [n]} \sum_{j_1, j_2 \in [n]} \epsilon_{m_1, m_2} \epsilon_{j_1, j_2} v_{j_1, j_2, l_3, l_4, l_5} (e_{l_5} \otimes e_{m_1} \otimes e_{l_4} \otimes e_{m_2} \otimes e_{l_3}) \quad (151)$$

This is the vector that is returned by **MatrixMult**.

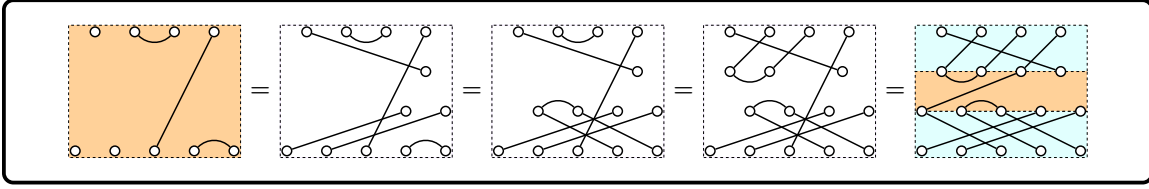


Figure 7: We use the string-like aspect of  $(l+k)\setminus n$ -diagrams to **Factor** them as a composition of a permutation in  $S_k$ , an algorithmically planar  $(l+k)\setminus n$ -diagram, and a permutation in  $S_l$ . Here,  $k=5$  and  $l=4$ .

**Time Complexity** The time complexity is exactly the same as for the orthogonal group.

#### 5.2.4 SPECIAL ORTHOGONAL GROUP $SO(n)$

We can perform matrix multiplication between either  $E_\beta$  or  $H_\alpha \in \text{Hom}_{SO(n)}((\mathbb{R}^n)^{\otimes k}, (\mathbb{R}^n)^{\otimes l})$  and  $v \in (\mathbb{R}^n)^{\otimes k}$ , where  $d_\beta$  is a  $(k, l)$ -Brauer diagram, and  $d_\alpha$  is an  $(l+k)\setminus n$ -diagram. Given that the implementation for the  $E_\beta$  case is the same as for the orthogonal group, by Theorem 11, we only consider the  $H_\alpha$  case below.

#### Implementation

**Factor:** The input is an  $(l+k)\setminus n$ -diagram  $d_\alpha$ . As before, we drag and bend the strings representing the connected components of  $d_\alpha$  to obtain a factoring of  $d_\alpha$  into the three diagrams, except this time the middle diagram will be an algorithmically planar  $(l+k)\setminus n$ -diagram.

To obtain the algorithmically planar  $(l+k)\setminus n$ -diagram we want to drag and bend the strings in any way such that

- the free vertices in the top row of  $d_\alpha$  are pulled down to the far right of the top row of the algorithmically planar  $(l+k)\setminus n$ -diagram, maintaining their order,
- the free vertices in the bottom row of  $d_\alpha$  are pulled up to the far right of the bottom row of the algorithmically planar  $(l+k)\setminus n$ -diagram, maintaining their order,
- the pairs in the bottom row of  $d_\alpha$  are pulled up to be next to each other in the right hand side of the bottom row of the algorithmically planar  $(l+k)\setminus n$ -diagram, but next to and to the left of the free vertices in the bottom row of the algorithmically planar  $(l+k)\setminus n$ -diagram,
- the pairs in the top row of  $d_\alpha$  are pulled down to be next to each other in the far left hand side of the top row of the algorithmically planar  $(l+k)\setminus n$ -diagram,
- the pairs connecting vertices in different rows of  $d_\alpha$  are ordered in the algorithmically planar  $(l+k)\setminus n$ -diagram in between the other vertices such that no two pairings in the algorithmically planar diagram intersect each other.

We give an example of this procedure in Figure 7.



**PlanarMult:** We take as input the algorithmically planar  $(l+k)\setminus n$ -diagram  $d_\alpha$  that is the output of **Factor**, and a vector  $v \in (\mathbb{R}^n)^{\otimes k}$  that is the output of **Permute**, as per Algorithm 1.

We need new subsets and notation to consider the impact of the free vertices in the  $(l+k)\setminus n$ -diagram  $d_\alpha$  on the implementation for **PlanarMult**.

As before, let  $t$  be the number of pairs that are solely in the top row of  $d_\alpha$ , let  $d$  be the number of pairs that are in different rows of  $d_\alpha$ , and let  $b$  be the number of pairs that are solely in the bottom row of  $d_\alpha$ . Now, let  $s$  be the number of free vertices in the top row of  $d_\alpha$ . Hence there are  $n-s$  free vertices in the bottom row of  $d_\alpha$ .

Then it is clear that

$$2t + d + s = l \quad \text{and} \quad 2b + d + n - s = k \quad (152)$$

and so

$$2t + 2d + 2b + n = l + k \quad (153)$$

Given how **Factor** constructs the algorithmically planar  $(l+k)\setminus n$ -diagram  $d_\alpha$ , the set partition  $\alpha$  corresponding to  $d_\alpha$  will be of the form

$$\left( \bigcup_{i=1}^t T_i \right) \cup \left( \bigcup_{i=1}^d D_i \right) \cup \left( \bigcup_{i=1}^s TF_i \right) \cup \left( \bigcup_{i=1}^b B_i \right) \cup \left( \bigcup_{i=1}^{n-s} BF_i \right) \quad (154)$$

where we have used  $T_i$  to refer to a top row pair,  $D_i$  to refer to a different row pair,  $TF_i$  to refer to a top row free vertex,  $B_i$  to refer to a bottom row pair, and  $BF_i$  to refer to a bottom row free vertex. In particular, we have that

- $T_i = \{2i-1, 2i\}$  for all  $i = 1 \rightarrow t$ ,
- $D_i = \{l+i-d-s, l+i\}$  for all  $i = 1 \rightarrow d$ ,
- $TF_i = \{l-s+i\}$  for all  $i = 1 \rightarrow s$ ,
- $B_i = \{l+d+2i-1, l+d+2i\}$  for all  $i = 1 \rightarrow b$ , and
- $BF_i = \{l+d+2b+i\}$  for all  $i = 1 \rightarrow n-s$ .

We take  $d_\alpha$  and express it as a tensor product of four types of set partition diagrams.

The right-most type is a diagram consisting of all the free vertices. Consequently, it corresponds to  $(\bigcup_{i=1}^s TF_i) \cup (\bigcup_{i=1}^{n-s} BF_i)$ . The type to its left is itself a tensor product of diagrams corresponding to the  $B_i$ ; the next type is a single diagram corresponding to  $(\bigcup_{i=1}^d D_i)$ ; and, finally, the left-most type is itself a tensor product of diagrams corresponding to the  $T_i$ .

We now apply the monoidal functor  $\Psi$  to this tensor product decomposition of diagrams, which returns a Kronecker product of matrices. We perform the matrix multiplication by applying the matrices “right-to-left, diagram-by-diagram”, as follows.

**Step 1: Apply the matrix that corresponds to the free vertices, that is, to  $(\bigcup_{i=1}^s TF_i) \cup (\bigcup_{i=1}^{n-s} BF_i)$ .**

The input will be a vector  $v \in (\mathbb{R}^n)^{\otimes k}$ .

As  $k = 2b + d + (n - s)$ , we can express  $v$  in the standard basis of  $\mathbb{R}^n$  as

$$v = \sum_{J \in [n]^{2b+d}} \sum_{B \in [n]^{n-s}} v_{J,B} e_{J,B} \quad (155)$$

This will be mapped to the vector  $w \in (\mathbb{R}^n)^{\otimes 2b+d+s}$ , where  $w$  is of the form

$$w = \sum_{J \in [n]^{2b+d}} \sum_{T \in [n]^s} w_{J,T} e_{J,T} \quad (156)$$

where

$$w_{J,T} = \sum_{B \in [n]^{n-s}} v_{J,B} \det(e_{T,B}) \quad (157)$$

**Step 2: Apply each matrix corresponding to a bottom row pair diagram, one-by-one, starting from the one that corresponds to  $B_b$  and ending with the one that corresponds to  $B_1$ .**

This is exactly the same as Step 1 for the orthogonal group. We obtain a vector  $y \in (\mathbb{R}^n)^{\otimes d+s}$

**Step 3: Now apply the matrix corresponding to the middle diagram, that is, to the set  $(\bigcup_{i=1}^d D_i)$ .**

This is exactly the same as Step 2 for the orthogonal group. We obtain a vector  $r := y \in (\mathbb{R}^n)^{\otimes d+s}$

**Step 4: Finally, apply each matrix corresponding to a top row pair diagram, one-by-one, starting from the one that corresponds to  $T_t$  and ending with the one that corresponds to  $T_1$ .**

This is exactly the same as Step 3 for the orthogonal group. We obtain a vector  $z \in (\mathbb{R}^n)^{\otimes 2t+d+s}$ . As  $2t + d + s = l$  by (152), we have that  $z \in (\mathbb{R}^n)^{\otimes l}$ , as required.

To summarise, the implementation of **PlanarMult** for  $SO(n)$  differs slightly from the implementation of **PlanarMult** for the groups that have come before. In the case where the spanning set element corresponds to a Brauer diagram, the implementation is the same as for the orthogonal group  $O(n)$ . Otherwise, the implementation takes as input the algorithmically planar  $(l + k) \setminus n$ -diagram that comes from **Factor**, but expresses it as a tensor product of *four* types of set partition diagrams. The right-most is a diagram consisting of all of the free vertices. This corresponds to the determinant map that is given in (32). The three other types of diagrams that appear in the decomposition and their corresponding operations are exactly the same as for the orthogonal group  $O(n)$ .

In Figure 8, we present an example of the tensor product decomposition for the algorithmically planar  $(4 + 5) \setminus 3$ -diagram given in Figure 7.

The diagrammatic representation of the matrix multiplication step is also very similar to the orthogonal group, in that to obtain the matrices we perform the same deformation of the tensor product decomposition of diagrams before applying the functor  $\Psi$ , defined in Theorem 30, at each level. Note, in particular, that we need to attach identity strings to the free vertices that appear in the top row.

We give an example in Figure 9 of how the computation takes place at each stage for the tensor product decomposition given in Figure 8, using its equivalent diagram form.

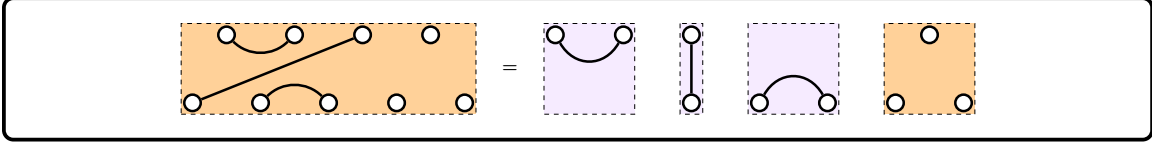


Figure 8: The tensor product decomposition of the algorithmically planar  $(4+5)\setminus 3$ -diagram that appears in Figure 7.

**Example 13** Suppose that we wish to perform the multiplication of  $H_\alpha$  by  $v \in (\mathbb{R}^3)^{\otimes 5}$ , where  $H_\alpha$  corresponds to the  $(4+5)\setminus 3$ -diagram  $d_\alpha$  given in Figure 7 under  $\Psi$ , and  $v$  is given by

$$\sum_{L \in [3]^5} v_L e_L \quad (158)$$

when expressed in the standard basis of  $\mathbb{R}^3$ .

We know that  $H_\alpha$  is a matrix in  $\text{Hom}_{SO(3)}((\mathbb{R}^3)^{\otimes 5}, (\mathbb{R}^3)^{\otimes 4})$ .

First, we apply the procedure **Factor**, which returns the three diagrams given in Figure 7. The first diagram corresponds to the permutation  $(13524)$  in  $S_5$ , hence, the result of **Permute** $(v, (13524))$  is the vector

$$\sum_{L \in [3]^5} v_{l_1, l_2, l_3, l_4, l_5} (e_{l_3} \otimes e_{l_4} \otimes e_{l_5} \otimes e_{l_1} \otimes e_{l_2}) \quad (159)$$

We now apply **PlanarMult** with the decomposition given in Figure 8.

Step 1: Apply the matrices that correspond to the free vertices.

We obtain the vector

$$w = \sum_{l_3, l_4, l_5, t_1 \in [3]} w_{l_3, l_4, l_5, t_1} (e_{l_3} \otimes e_{l_4} \otimes e_{l_5} \otimes e_{t_1}) \quad (160)$$

where

$$w_{l_3, l_4, l_5, t_1} = \sum_{l_1, l_2 \in [3]} v_{l_1, l_2, l_3, l_4, l_5} \det(e_{t_1} \otimes e_{l_1} \otimes e_{l_2}) \quad (161)$$

Step 2: Apply the matrices that correspond to the bottom row pairs.

We obtain the vector

$$y = \sum_{l_3, t_1 \in [3]} y_{l_3, t_1} (e_{l_3} \otimes e_{t_1}) \quad (162)$$

where

$$y_{l_3, t_1} = \sum_{j \in [3]} w_{l_3, j, j, t_1} \quad (163)$$

Step 3: Apply the matrices that correspond to the different row pairs.

Here, we get that  $r = y$ , as the transfer operations correspond to the identity.

Step 4: Apply the matrices that correspond to the top row pairs.

We obtain the vector

$$z = \sum_{m \in [3]} \sum_{l_3, t_1 \in [3]} y_{l_3, t_1} (e_m \otimes e_m \otimes e_{l_3} \otimes e_{t_1}) \quad (164)$$

Substituting in, we get that

$$z = \sum_{m \in [3]} \sum_{l_3, t_1 \in [3]} \sum_{j \in [3]} w_{l_3, j, j, t_1} (e_m \otimes e_m \otimes e_{l_3} \otimes e_{t_1}) \quad (165)$$

and hence

$$z = \sum_{m \in [3]} \sum_{l_3, t_1 \in [3]} \sum_{j \in [3]} \sum_{l_1, l_2 \in [3]} v_{l_1, l_2, l_3, j, j} \det(e_{t_1} \otimes e_{l_1} \otimes e_{l_2}) (e_m \otimes e_m \otimes e_{l_3} \otimes e_{t_1}) \quad (166)$$

Finally, as the third diagram returned from **Factor** corresponds to the permutation (1432) in  $S_4$ , we perform **Permute**( $z, (1432)$ ) which returns the vector

$$\sum_{m \in [3]} \sum_{l_3, t_1 \in [3]} \sum_{j \in [3]} \sum_{l_1, l_2 \in [3]} v_{l_1, l_2, l_3, j, j} \det(e_{t_1} \otimes e_{l_1} \otimes e_{l_2}) (e_{t_1} \otimes e_m \otimes e_m \otimes e_{l_3}) \quad (167)$$

This is the vector that is returned by **MatrixMult**.

**Time Complexity** For a matrix corresponding to a  $(k, l)$ -Brauer diagram, the analysis is the same as for the orthogonal group. For a matrix corresponding to an  $(l+k) \setminus n$ -diagram, we look at each step of the implementation that was given above.

**Step 1:** Recall that we map a vector in  $(\mathbb{R}^n)^{\otimes k}$  to a vector in  $(\mathbb{R}^n)^{\otimes 2b+d+s}$  in this step.

To obtain the best time complexity, we need to look at the tuples  $J \in [n]^{2b+d}$ ,  $T \in [n]^s$  and  $B \in [n]^{n-s}$  that appear in (155), (156), and (157).

Indeed, for each tuple  $J$ , we first need to consider how many tuples  $T$  come with pairwise different entries in  $[n]$ . The number of such tuples is  $\frac{n!}{(n-s)!}$ . Consequently, we only need to perform multiplications and additions for entries with such indices  $(J, T)$ . Let us call any such pair of indices  $(J, T)$  **valid**.

Hence, for each valid tuple  $(J, T)$ , there are  $(n-s)!$  multiplications and  $(n-s)! - 1$  additions. Since the number of valid tuples of the form  $(J, T)$  is

$$n^{2b+d} \frac{n!}{(n-s)!} \quad (168)$$

we have that the overall time complexity is  $O(n^{k-(n-s)}n!)$  for this step, since  $2b+d = k - (n-s)$  by (152).

**Step 2:** By the operations performed in this step, we can immediately apply the analysis of Step 1 for the orthogonal group.

Since the part of the matrix multiplication that corresponds to  $B_i$ , for some  $i = 1 \rightarrow b$ , maps a vector in  $(\mathbb{R}^n)^{\otimes d+s+2i}$  to a vector in  $(\mathbb{R}^n)^{\otimes d+s+2i-2}$ , we have that the overall time complexity is  $O(n^{k+s-(n-s)-1})$  for this step, since  $2b+d+s = k+s-(n-s)$  by (152).

**Steps 3, 4:** These steps correspond to Steps 2, 3 for the orthogonal group, hence they have no cost.

Hence, we have reduced the overall time complexity from  $O(n^{l+k})$  to

$$O(n^{k-(n-s)}(n! + n^{s-1})) \quad (169)$$

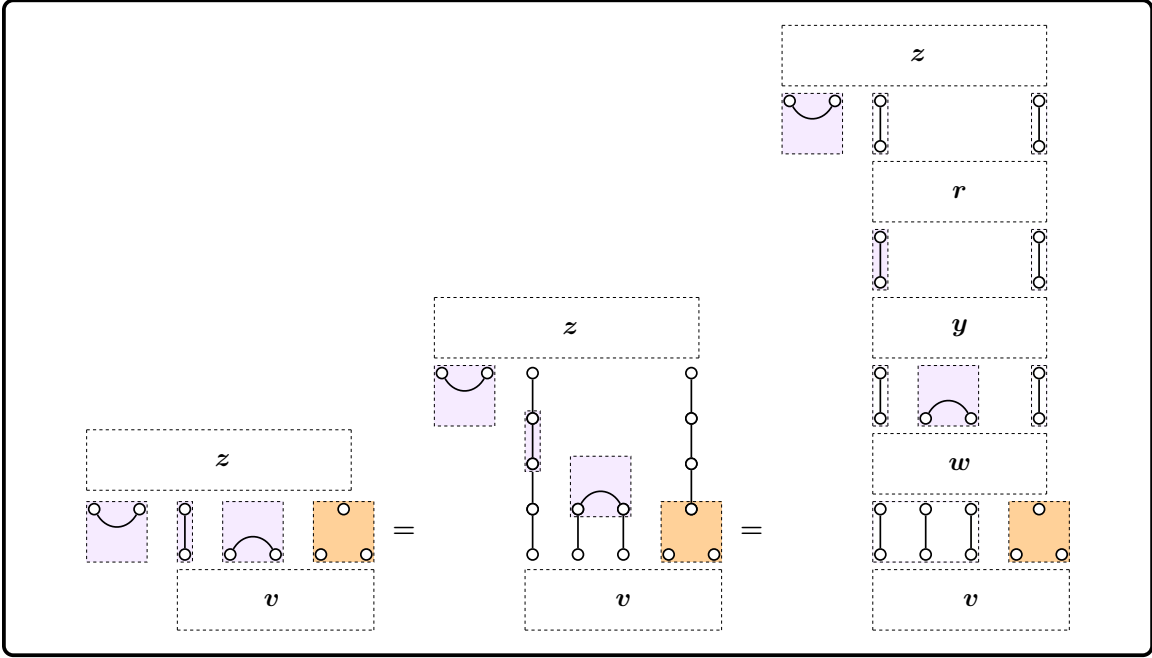


Figure 9: We show how matrix multiplication is implemented in **PlanarMult** for  $SO(n)$  (here  $n = 3$ ) using the tensor product decomposition of the algorithmically planar  $(4 + 5)3$ -diagram given in Figure 8 as an example. We perform the matrix multiplication as follows: first, we deform the entire tensor product decomposition diagram by pulling each individual diagram up one level higher than the previous one, going from right-to-left, and then we apply the functor  $\Psi$  at each level. Note, in particular, that we need to attach identity strings to the free vertices appearing in the top row. Finally, we perform matrix multiplication at each level to obtain the final output vector.

## 6 Conclusion

Group equivariant neural networks that use high-order tensor power spaces of  $\mathbb{R}^n$  as their layers often face prohibitively high computational costs when an equivariant weight matrix is applied to an input vector. In this work, we have developed an algorithm that improves upon a naïve weight matrix multiplication exponentially in terms of its Big- $O$  time complexity for four groups: the symmetric, orthogonal, special orthogonal and symplectic groups. We showed that a category-theoretic framework – namely, expressing each weight matrix as the image of a linear combination of diagrams under a monoidal functor – was very effective in helping to reorganise the overall computation so that it can be executed in an optimal manner. We hope that our algorithm will encourage more widespread adoption of group equivariant neural networks that use high-order tensor power spaces in practical applications.

## Acknowledgments and Disclosure of Funding

This work was funded by the Doctoral Scholarship for Applied Research which was awarded to the first author under Imperial College London’s Department of Computing Applied Research scheme. This work will form part of the first author’s PhD thesis at Imperial College London.

## References

- V. Abbott. Neural Circuit Diagrams: Robust Diagrams for the Communication, Implementation, and Analysis of Deep Learning Architectures. *Transactions on Machine Learning Research*, 2024.
- G. Benkart and T. Halverson. Partition algebras  $P_k(n)$  with  $2k > n$  and the fundamental theorems of invariant theory for the symmetric group  $S_n$ . *Journal of the London Mathematical Society*, 99(2):194–224, 2019a.
- G. Benkart and T. Halverson. Partition Algebras and the Invariant Theory of the Symmetric Group. In *Recent Trends in Algebraic Combinatorics*, volume 16 of *Association for Women in Mathematics Series*, pages 1–41. Springer, 2019b.
- G. Benkart, T. Halverson, and N. Harman. Dimensions of irreducible modules for partition algebras and tensor power multiplicities for symmetric and alternating groups. *Journal of Algebraic Combinatorics. An International Journal*, 46(1):77–108, 2017.
- B. Bloem-Reddy and Y. W. Teh. Probabilistic Symmetries and Invariant Neural Networks. *Journal of Machine Learning Research*, 21:1–61, 2020.
- A. Bogatskiy, B. Anderson, J. Offermann, M. Roussi, D. Miller, and R. Kondor. Lorentz Group Equivariant Neural Network for Particle Physics. In *International Conference on Machine Learning*, pages 992–1002. PMLR, 2020.
- R. Brauer. On Algebras Which Are Connected with the Semisimple Continuous Groups. *Annals of Mathematics*, 38:857–872, 1937.
- W. P. Brown. An Algebra Related to the Orthogonal Group. *Michigan Mathematical Journal*, 3(1):1 – 22, 1955.
- W. P. Brown. The Semisimplicity of the Brauer Algebra. *Annals of Mathematics*, 63(2): 324–335, 1956.
- E. Chatzipantazis, S. Pertigkiozoglou, E. Dobriban, and K. Daniilidis. SE(3)-Equivariant Attention Networks for Shape Reconstruction in Function Space. In *The Eleventh International Conference on Learning Representations*, 2023.
- K. Cho and B. Jacobs. Disintegration and Bayesian inversion via string diagrams. *Mathematical Structures in Computer Science*, 29(7):938–971, 2019.
- B. Coecke and A. Kissinger. *Picturing Quantum Processes: A First Course in Quantum Theory and Diagrammatic Reasoning*. Cambridge University Press, 2017.

- T. Cohen and M. Welling. Group Equivariant Convolutional Networks. In *Proceedings of The 33rd International Conference on Machine Learning*, volume 48 of *Proceedings of Machine Learning Research*, pages 2990–2999, New York, USA, 20–22 Jun 2016. PMLR.
- T. Cohen and M. Welling. Steerable CNNs. In *International Conference on Learning Representations*, 2017.
- T. Cohen, M. Geiger, J. Köhler, and M. Welling. Spherical CNNs. In *International Conference on Learning Representations*, 2018.
- T. Cohen, M. Geiger, and M. Weiler. A General Theory of Equivariant CNNs on Homogeneous Spaces. In *Advances in Neural Information Processing Systems*, volume 32, 2019.
- J. Comes. Jellyfish Partition Categories. *Algebras and Representation Theory*, 23:327–347, 2020.
- R. Cornish. Stochastic Neural Network Symmetrisation in Markov Categories, 2024. [arXiv:2406.11814](https://arxiv.org/abs/2406.11814).
- G. Cruttwell, B. Gavranović, N. Ghani, P. Wilson, and F. Zanasi. Categorical Foundations of Gradient-Based Learning. In I. Sergey, editor, *Programming Languages and Systems*, volume 13240 of *Lecture Notes in Computer Science*. Springer, Cham, 2022.
- P. de Haan, T. S. Cohen, and M. Welling. Natural Graph Networks. In *Advances in Neural Information Processing Systems*, volume 33, pages 3636–3646, 2020.
- R. Duncan, A. Kissinger, S. Perdrix, and J. van de Wetering. Graph-theoretic Simplification of Quantum Circuits with the ZX-calculus. *Quantum*, 4, June 2020.
- C. Esteves, C. Allen-Blanchette, A. Makadia, and K. Daniilidis. Learning  $SO(3)$  Equivariant Representations with Spherical CNNs. In *Proceedings of the European Conference on Computer Vision (ECCV)*, pages 52–68, 2018.
- M. Finzi, M. Welling, and A. G. Wilson. A Practical Method for Constructing Equivariant Multilayer Perceptrons for Arbitrary Matrix Groups. In *Proceedings of the 38th International Conference on Machine Learning*, volume 139 of *Proceedings of Machine Learning Research*, pages 3318–3328. PMLR, 18–24 Jul 2021.
- T. Fritz. A synthetic approach to Markov kernels, conditional independence and theorems on sufficient statistics. *Advances in Mathematics*, 370:107239, 2020.
- B. Gavranović, P. Lessard, A. J. Dudzik, T. Von Glehn, J. a. G. Madeira Araújo, and P. Veličković. Position: Categorical Deep Learning is an Algebraic Theory of All Architectures. In *Proceedings of the 41st International Conference on Machine Learning*, volume 235 of *Proceedings of Machine Learning Research*, pages 15209–15241. PMLR, 21–27 Jul 2024.
- C. Godfrey, M. G. Rawson, D. Brown, and H. Kvinge. Fast computation of permutation equivariant layers with the partition algebra. In *ICLR 2023 Workshop on Physics for Machine Learning*, 2023.

- J. Gordon, D. Lopez-Paz, M. Baroni, and D. Bouchacourt. Permutation Equivariant Models for Compositional Generalization in Language. In *International Conference on Learning Representations*, 2020.
- C. Groot. Brauer Algebras and Centralizer Algebras for  $SO(2n, \mathbb{C})$ . *Journal of Algebra*, 222(2):678–707, 1999.
- N. Guttenberg, N. Virgo, O. Witkowski, H. Aoki, and R. Kanai. Permutation-equivariant neural networks applied to dynamics prediction, 2016. [arXiv:1612.04530](https://arxiv.org/abs/1612.04530).
- T. Halverson and A. Ram. Gems from the Work of Georgia Benkart. *Notices of the American Mathematical Society*, 69(3):375–384, 2022.
- P. Hanlon and D. Wales. On the Decomposition of Brauer’s Centralizer Algebras. *Journal of Algebra*, 121(2):409–445, 1989.
- J. S. Hartford, D. R. Graham, K. Leyton-Brown, and S. Ravanbakhsh. Deep Models of Interactions Across Sets. In *Proceedings of the 35th International Conference on Machine Learning*, pages 1914–1923. PMLR, 2018.
- C. Heunen and J. Vicary. *Categories for Quantum Theory: An Introduction*. Oxford University Press, 2020.
- M. Hu. Presentations of Diagram Categories. *The PUMP Journal of Undergraduate Research*, 3:1–25, 2019.
- V. F. R. Jones. The Potts model and the symmetric group. In *Subfactors: Proceedings of the Taniguchi Symposium on Operator Algebras (Kyuzeso, 1993)*, pages 259–267. World Scientific, 1994.
- J. Jumper, R. Evans, A. Pritzel, T. Green, M. Figurnov, O. Ronneberger, K. Tunyasuvunakool, R. Bates, A. Žídek, A. Potapenko, A. Bridgland, C. Meyer, S. A. A. Kohl, A. J. Ballard, A. Cowie, B. Romera-Paredes, S. Nikolov, R. Jain, J. Adler, T. Back, S. Petersen, D. Reiman, E. Clancy, M. Zielinski, M. Steinegger, M. Pacholska, T. Berghammer, S. Bodenstein, D. Silver, O. Vinyals, A. W. Senior, K. Kavukcuoglu, P. Kohli, and D. Hassabis. Highly accurate protein structure prediction with AlphaFold. *Nature*, 596(7873):583–589, 2021.
- N. Khatri, T. Laakkonen, J. Liu, and V. Wang-Maścianica. On the Anatomy of Attention, 2024. [arXiv:2407.02423](https://arxiv.org/abs/2407.02423).
- A. Kissinger. Pictures of processes: Automated graph rewriting for monoidal categories and applications to quantum computing, 2012. [arXiv:1203.0202](https://arxiv.org/abs/1203.0202).
- J. Kock. *Frobenius Algebras and 2-D Topological Quantum Field Theories*. London Mathematical Society Student Texts. Cambridge University Press, 2003.
- R. Kondor and S. Trivedi. On the Generalization of Equivariance and Convolution in Neural Networks to the Action of Compact Groups. In *Proceedings of the 35th International Conference on Machine Learning*, volume 80 of *Proceedings of Machine Learning Research*, pages 2747–2755. PMLR, 10–15 Jul 2018.



- R. Kondor, Z. Lin, and S. Trivedi. Clebsch–Gordan Nets: a Fully Fourier Space Spherical Convolutional Neural Network. In *Advances in Neural Information Processing Systems*, volume 31, 2018.
- A. D. Lauda and J. Sussan. An Invitation to Categorification. *Notices of the American Mathematical Society*, 69(1):11–21, 2022.
- G. I. Lehrer and R. B. Zhang. The Brauer category and invariant theory. *Journal of the European Mathematical Society*, 17:2311–2351, 2012.
- G. I. Lehrer and R. B. Zhang. Invariants of the special orthogonal group and an enhanced Brauer category. *L’Enseignement Mathématique*, 63:181–200, 2018.
- T. Leinster. *Basic Category Theory*. Cambridge University Press, 2014.
- R. Lorenz and S. Tull. Causal models in string diagrams, 2023. [arXiv:2304.07638](https://arxiv.org/abs/2304.07638).
- S. Mac Lane. *Categories for the Working Mathematician*. Springer New York, NY, 1998.
- H. Maron, H. Ben-Hamu, N. Shamir, and Y. Lipman. Invariant and Equivariant Graph Networks. In *International Conference on Learning Representations*, 2019a.
- H. Maron, E. Fetaya, N. Segol, and Y. Lipman. On the Universality of Invariant Networks. In *Proceedings of the 36th International Conference on Machine Learning*, volume 97 of *Proceedings of Machine Learning Research*, pages 4363–4371. PMLR, 09–15 Jun 2019b.
- H. Maron, O. Litany, G. Chechik, and E. Fetaya. On Learning Sets of Symmetric Elements. In *Proceedings of the 37th International Conference on Machine Learning*, volume 119 of *Proceedings of Machine Learning Research*, pages 6734–6744. PMLR, 13–18 Jul 2020.
- P. P. Martin. Representations of Graph Temperley–Lieb Algebras. *Publications of the Research Institute for Mathematical Sciences*, 26(3):485–503, 1990.
- P. P. Martin. Temperley–Lieb Algebras for Non–Planar Statistical Mechanics – the Partition Algebra Construction. *Journal of Knot Theory and Its Ramifications*, 03(01):51–82, 1994.
- P. P. Martin. The Structure of the Partition Algebras. *Journal of Algebra*, 183:319–358, 1996.
- H. Pan and R. Kondor. Permutation Equivariant Layers for Higher Order Interactions. In *Proceedings of The 25th International Conference on Artificial Intelligence and Statistics*, volume 151 of *Proceedings of Machine Learning Research*, pages 5987–6001. PMLR, 28–30 Mar 2022.
- E. Pearce-Crump. Brauer’s Group Equivariant Neural Networks. In *Proceedings of the 40th International Conference on Machine Learning*, volume 202 of *Proceedings of Machine Learning Research*, pages 27461–27482. PMLR, 23–29 Jul 2023a.
- E. Pearce-Crump. How Jellyfish Characterise Alternating Group Equivariant Neural Networks. In *Proceedings of the 40th International Conference on Machine Learning*, volume 202 of *Proceedings of Machine Learning Research*, pages 27483–27495. PMLR, 23–29 Jul 2023b.

- E. Pearce-Crump. Connecting Permutation Equivariant Neural Networks and Partition Diagrams. In *Proceedings of the 27th European Conference on Artificial Intelligence (ECAI 2024)*, volume 392 of *Frontiers in Artificial Intelligence and Applications*, pages 1511–1518. IOS Press, 2024.
- E. Pearce-Crump and W. Knottenbelt. Graph Automorphism Group Equivariant Neural Networks. In *Proceedings of the 41st International Conference on Machine Learning*, volume 235 of *Proceedings of Machine Learning Research*, pages 40051–40077. PMLR, 21–27 Jul 2024.
- M. Petrache and S. Trivedi. Position Paper: Generalized Grammar Rules and Structure-Based Generalization Beyond Classical Equivariance for Lexical Tasks and Transduction, 2024. [arXiv:2402.01629](https://arxiv.org/abs/2402.01629).
- C. R. Qi, H. Su, K. Mo, and L. J. Guibas. PointNet: Deep Learning on Point Sets for 3D Classification and Segmentation. In *Proceedings of the IEEE Conference on Computer Vision and Pattern Recognition*, pages 652–660, 2017.
- J. Rahme, S. Jelassi, J. Bruna, and S. M. Weinberg. A Permutation-Equivariant Neural Network Architecture For Auction Design. *Proceedings of the AAAI Conference on Artificial Intelligence*, 35(6):5664–5672, 2021.
- S. Ravanbakhsh, J. Schneider, and B. Póczos. Equivariance Through Parameter-Sharing. In *Proceedings of the 34th International Conference on Machine Learning*, volume 70, pages 2892–2901, 06–11 Aug 2017.
- E. Riehl. *Category Theory in Context*. Dover Publications, 2017.
- V. G. Satorras, E. Hoogeboom, and M. Welling. E(n) Equivariant Graph Neural Networks. In *Proceedings of the 38th International Conference on Machine Learning*, volume 139 of *Proceedings of Machine Learning Research*, pages 9323–9332. PMLR, 18–24 Jul 2021.
- A. Savage. *String Diagrams and Categorification*, pages 3–36. Springer International Publishing, 2021.
- N. Thomas, T. Smidt, S. Kearnes, L. Yang, L. Li, K. Kohlhoff, and P. Riley. Tensor field networks: Rotation- and translation-equivariant neural networks for 3d point clouds, 2018. [arXiv:1802.08219](https://arxiv.org/abs/1802.08219).
- S. Tull, R. Lorenz, S. Clark, I. Khan, and B. Coecke. Towards Compositional Interpretability for XAI, 2024. [arXiv:2406.17583](https://arxiv.org/abs/2406.17583).
- V. Turaev and A. Virelizier. *Monoidal Categories and Topological Field Theory*. Birkhäuser, 2017.
- J. van de Wetering. ZX-calculus for the working quantum computer scientist, 2020. [arXiv:2012.13966](https://arxiv.org/abs/2012.13966).
- S. Villar, D. W. Hogg, K. Storey-Fisher, W. Yao, and B. Blum-Smith. Scalars are universal: Equivariant machine learning, structured like classical physics. In *Advances in Neural Information Processing Systems*, 2021.

- M. Weiler and G. Cesa. General  $E(2)$ -Equivariant Steerable CNNs. In *Advances in Neural Information Processing Systems*, volume 32, 2019.
- H. Wenzl. On the Structure of Brauer’s Centralizer Algebras. *Annals of Mathematics*, 128 (1):173–193, 1988.
- H. Weyl. *The Classical Groups: Their Invariants and Representations*. Princeton University Press, 1939.
- M. Zaheer, S. Kottur, S. Ravanbakhsh, B. Póczos, R. R. Salakhutdinov, and A. J. Smola. Deep Sets. In *Advances in Neural Information Processing Systems*, volume 30, 2017.